SMC-TR-93-24

AEROSPACE REPORT NO.
TR-93(3935)-4

Applications of Surface Science to Solid Lubricants

Prepared by

S. V. DIDZIULIS and P. D. FLEISCHAUER
Mechanics and Materials Technology Center
Technology Operations

15 March 1993

Prepared for

SPACE AND MISSILE SYSTEMS CENTER
AIR FORCE MATERIEL COMMAND
Los Angeles Air Force Base
P. O. Box 92960
Los Angeles, CA 90009-2960

Engineering and Technology Group

THE AEROSPACE CORPORATION
El Segundo, California

This report was submitted by The Aerospace Corporation, El Segundo, CA 90245-4691, under Contract No. F04701-88-C-0089 with the Space and Missile Systems Center, P. O. Box 92960, Los Angeles, CA 90009-2960. It was reviewed and approved for The Aerospace Corporation by R. W. Fillers, Principal Director, Mechanics and Materials Technology Center. Capt. Mark Borden was the project officer.

This report has been reviewed by the Public Affairs Office (PAS) and is releasable to the National Technical Information Service (NTIS). At NTIS, it will be available to the general public, including foreign nationals.

This technical report has been reviewed and is approved for publication. Publication of this report does not constitute Air Force approval of the report's findings or conclusions. It is published only for the exchange and stimulation of ideas.

MARK W. BORDEN, Captain, USAF
MOIE Monitor

W. KYLE SNEDDON, Capt., USAF
MOIE Program Manager

UNCLASSIFIED

SECURITY CLASSIFICATION OF THIS PAGE

REPORT DOCUMENTATION PAGE

1a. REPORT SECURITY CLASSIFICATION Unclassified	1b. RESTRICTIVE MARKINGS
2a. SECURITY CLASSIFICATION AUTHORITY	3. DISTRIBUTION/AVAILABILITY OF REPORT Approved for public release; distribution unlimited
2b. DECLASSIFICATION/DOWNGRADING SCHEDULE	
4. PERFORMING ORGANIZATION REPORT NUMBER(S) TR-93(3935)-4	5. MONITORING ORGANIZATION REPORT NUMBER(S) SMC-TR-93-24
6a. NAME OF PERFORMING ORGANIZATION The Aerospace Corporation Technology Operations 6b. OFFICE SYMBOL *(If applicable)*	7a. NAME OF MONITORING ORGANIZATION Space and Missile Systems Center
6c. ADDRESS *(City, State, and ZIP Code)* El Segundo, CA 90245-4691	7b. ADDRESS *(City, State, and ZIP Code)* Los Angeles Air Force Base Los Angeles, CA 90009-2960
8a. NAME OF FUNDING/SPONSORING ORGANIZATION 8b. OFFICE SYMBOL *(If applicable)*	9. PROCUREMENT INSTRUMENT IDENTIFICATION NUMBER F04701-88-C-0089
8c. ADDRESS *(City, State, and ZIP Code)*	10. SOURCE OF FUNDING NUMBERS PROGRAM ELEMENT NO. / PROJECT NO. / TASK NO. / WORK UNIT ACCESSION NO.

11. TITLE *(Include Security Classification)*
Applications of Surface Science to Solid Lubricants

12. PERSONAL AUTHOR(S)
Didziulis, Stephen V.; Fleischauer, Paul D.

13a. TYPE OF REPORT	13b. TIME COVERED FROM ____ TO ____	14. DATE OF REPORT *(Year, Month, Day)*	15. PAGE COUNT
		1993 March 15	57

16. SUPPLEMENTARY NOTATION

17. COSATI CODES			18. SUBJECT TERMS *(Continue on reverse if necessary and identify by block number)*
FIELD	GROUP	SUB-GROUP	Tribology, Solid Lubricants, Surface Science, Surface Chemistry, Synchrotron Radiation, Photoelectron Spectroscopy, Molybdenum Disulfide

19. ABSTRACT *(Continue on reverse if necessary and identify by block number)*

Solid lubricants fill a very important niche in the world of tribology by providing low-friction surfaces under harsh operating conditions, such as high or very low temperature and high vacuum. The successful use of solid lubricants in most applications relies on controlling the chemical interactions occurring at several interfaces, and the use of surface science techniques to study and understand these chemical interactions has become increasingly more important in recent years. In this report, the surface properties of molybdenum disulfide (MoS_2), the most widely used solid lubricant for space applications, are studied with a variety of techniques.

The techniques discussed are: valence band photoelectron spectroscopy (PES) to determine electronic structure properties; scanning tunneling and atomic force microscopies to examine surface structure; high-resolution electron energy loss spectroscopy to determine surface phonon properties; core level PES with synchrotron radiation to study metal/MoS_2 interfacial chemistry; core level X-ray photoelectron spectroscopy to study steel and ceramic substrate chemistry; and extended X-ray absorption fine structure, electron microscopies, and X-

20. DISTRIBUTION/AVAILABILITY OF ABSTRACT	21. ABSTRACT SECURITY CLASSIFICATION
[X] UNCLASSIFIED/UNLIMITED [ ] SAME AS RPT. [ ] DTIC USERS	Unclassified

22a. NAME OF RESPONSIBLE INDIVIDUAL	22b. TELEPHONE *(Include Area Code)*	22c. OFFICE SYMBOL

DD FORM 1473, 84 MAR

83 APR edition may be used until exhausted.
All other editions are obsolete.

SECURITY CLASSIFICATION OF THIS PAGE
UNCLASSIFIED

ray diffraction to study film structure. In addition, theoretical and tribological studies of MoS_2 are discussed. The goal of this work is to develop a fundamental understanding of the electronic structure and reactivity of MoS_2 as determined by these surface science techniques, and to relate this fundamental understanding to the performance of MoS_2 as a solid lubricant.

PREFACE

This report was originally prepared as a chapter for a book entitled "Review Volume in Surface Science and Tribology," edited by Dr. Kazuhisa Miyoshi of the NASA Lewis Research Center. The report reviews work on the solid lubricant molybdenum disulfide (MoS_2) that has been performed at The Aerospace Corporation and other institutions. The Aerospace personnel that originally performed much of the work described should be acknowledged. They are Dr. Jeffrey R. Lince, Dr. Michael R. Hilton, Reinhold Bauer, Dr. P. Ann Bertrand, Thomas B. Stewart, Thomas D. Durbin, Dr. Gary W. Stupian, Dr. Martin S. Leung, Neil Ives, Dr. David J. Carré, Dr. Malina M. Mills, Sandra Jackson, and Jeffrey Childs.

This report represents the compilation of many years of work on MoS_2, and we gratefully acknowledge the technical guidance provided by Dr. H. K. Alan Kan throughout this research program. Finally, work on solid lubrication and MoS_2-based materials continues today, both on fundamental issues and the use of these lubricants in spacecraft mechanisms. Much of the understanding that we have obtained on MoS_2 is based on the work described in this report.

CONTENTS

FIGURES

1. INTRODUCTION

Tribology (the science of friction, wear, and lubrication) is all about surfaces. Contact of two objects in relative motion, be it rolling, sliding, or a combination of the two, involves the interaction of a number of different surfaces or interfaces. Whereas some "interfaces" in fluid lubricated systems may be constantly changing structure (e.g., flowing in hydrodynamic lubrication) and therefore relatively difficult to characterize, those involved in solid-film lubrication comprise fairly distinct and tractable arrangements with relatively stable compositions and structures. Consequently, the surface chemistries of these interfaces can be quite accurately defined and investigated. In this report, we will use a description of the lubricant interface patterned after Braithwaite [1] and further refined by Gardos [2] to provide a framework for describing surface structure and chemistry, namely, that of a progression from a bulk material to a solid lubricant film and on to a second bulk solid as depicted in Figure 1.

The interfaces described by this picture include (1) grain boundaries within the bulk substrates, (2) the region between bulk metal or ceramic and any oxide or other passivation film, (3) that between the oxide and the solid lubricant film, and (4) the intercrystalline grain boundaries and shear planes within the thin-film lubricant layer. (The question of whether the total system is symmetrical with respect to an inversion plane through the lubricant film will be addressed in Sections 4 and 5 on Film Structure and Tribology Studies.) It is clear that a veritable plethora of surface science exists for this type of materials system, and that surface properties and conditions (composition, bonding, geometries, etc.) control system performance, namely, the friction and wear properties.

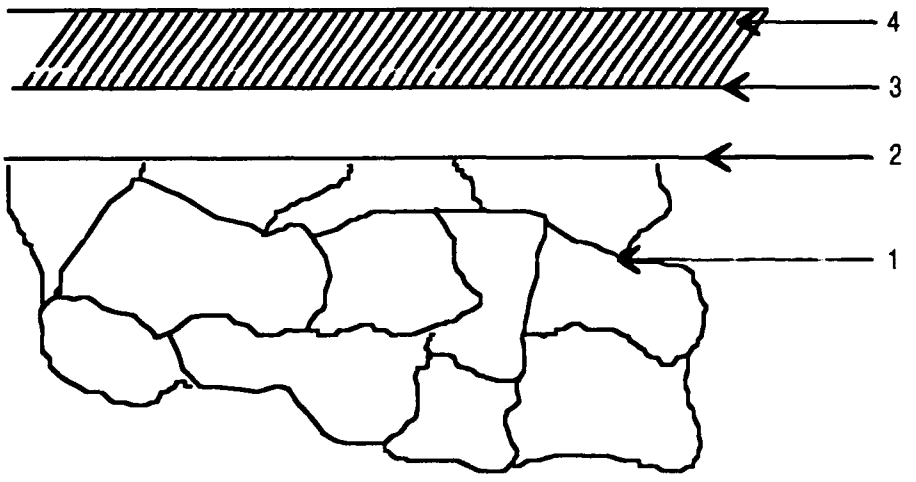

Figure 1. A schematic diagram showing the various interfaces present in a solid lubricated surface region. The interfaces are: (1) bulk substrate intergranular interfaces, (2) substrate bulk-oxide, (3) substrate surface oxide-solid lubricant, and (4) solid lubricant intergranular.

1.1 SOLID LUBRICANT DEFINITION

Our system description presupposes both a definition and certain properties of a solid lubricant. Others have defined lubrication in general and solid lubricants in particular. Braithwaite [1] defines lubrication as the "reduction of friction or wear between two relatively moving surfaces in contact" and a solid lubricant as "a material that will separate two moving surfaces under boundary conditions and decrease the amount of wear." Lancaster [3] defines a solid lubricant as "any material used as a powder or a thin film on a surface to provide protection from damage during relative movement and to reduce friction and wear." Bowden and Tabor lean toward classical discussions of friction by citing Leonardo da Vinci, Amontons, and Coulomb [4]. They discuss the mechanism of friction in terms of shearing and ploughing terms, concluding that the former is dominant. It follows then that a good solid lubricant is one that reduces the forces required to generate shear between two contacting bodies.

In our discussion of the surface science of solid lubricants, we will be rather more selective in scope. As implied above, we will deal with thin lubricant films, meaning those at the micrometer or less scale, that are primarily prepared by physical vapor deposition, although some discussion of burnishing and mechanically transferred films will be included. Further, because many of the basic surface science principles involved in solid lubrication are common to practically all systems, we will select one class of materials that also has unique properties resulting from their particular atomic (crystal) structure, namely, the layered lattice materials represented by MoS_2. Before concentrating on this very unusual and versatile material, however, some general discussion of solid lubricants and the wider topic of their surface properties will be presented. Subsequently, aspects of electronic structure, surface reactivity, film structure, and tribological activity of MoS_2 systems will be described.

1.2 BASIC PROPERTIES OF SOLID LUBRICANTS

Solid lubricants fulfill a technologically important role as materials that can function in harsh environments to provide extremely low coefficients of friction. They typically have no measurable vapor pressure so they can operate in vacuum or under conditions where volatile constituents could otherwise be a detriment, as in aerospace applications that cannot tolerate condensation of contaminant films on critical surfaces (e.g., sensitive optics). They function equally well at very low (down to 20 K or lower) or relatively high temperatures (some in excess of 1000 K) and generally are not degraded by energetic radiation, making them desirable for use on satellites and space-based mechanisms, as well as in nuclear reactors.

Solid lubricants are applied to a surface either by some type of precoating process or by continuous rubbing of a sacrificial reservoir of material, such as a ball-bearing retainer. Sometimes they are transferred from one surface to a counter surface during operation. (Another method of generating solid lubricant films, by reacting a gas *in situ* to create a conversion layer, though fraught with surface chemical interactions, is beyond the scope of this report [5].) In any case, it is essential that the lubricant remain in the area between the contacting surfaces in order to be effective. Unlike fluids (oils or gases) that can redistribute easily during operation to re-coat depleted surfaces, solids need to bond to a surface and remain there, or they need to be replenished by some type of contact process. Therefore, the chemical and physical interactions (surface science) between the surfaces of the lubricant and the substrates are absolutely critical to proper function of the lubricated systems.

Ideally, a solid lubricant needs to be thick enough to affect the shear properties of contacting surfaces but not so thick as to alter their load bearing capacities, fracture strengths, or gross deformation processes. Most solids lubricate because they deform more readily than the load bearing elements. However, the nature of the deformation processes is governed by chemical and electronic properties of the materials that, in turn, determine the atomic arrangements and crystalline structural features of the solid (which can be very short range as will be discussed below). MoS_2 is probably the most graphic example of the significance of electronic structure on overall lubrication ability [6,7] MoS_2 is one of a number of layered solids (its structure is shown in Figure 2), but one in which the layers appear to be held together by the weakest of forces, and yet it does maintain its shape. Its ability to lubricate depends on the fact that the reactivity of its basal planes is essentially nil so that they can slide over each other with little or no resistance (i.e., provide low shear force). However, for optimum performance, it should be bonded to the surfaces to be lubricated through reaction of these same basal planes. The implications of this "paradox" have been the subject of numerous scientific and practical investigations [8-12], and a reasonable picture of the mechanism by which the material functions is beginning to emerge. It is emphasized that this understanding is forthcoming from the results of surface science studies, both spectroscopic investigations of electronic structure and bonding and microscopic examinations of atomic

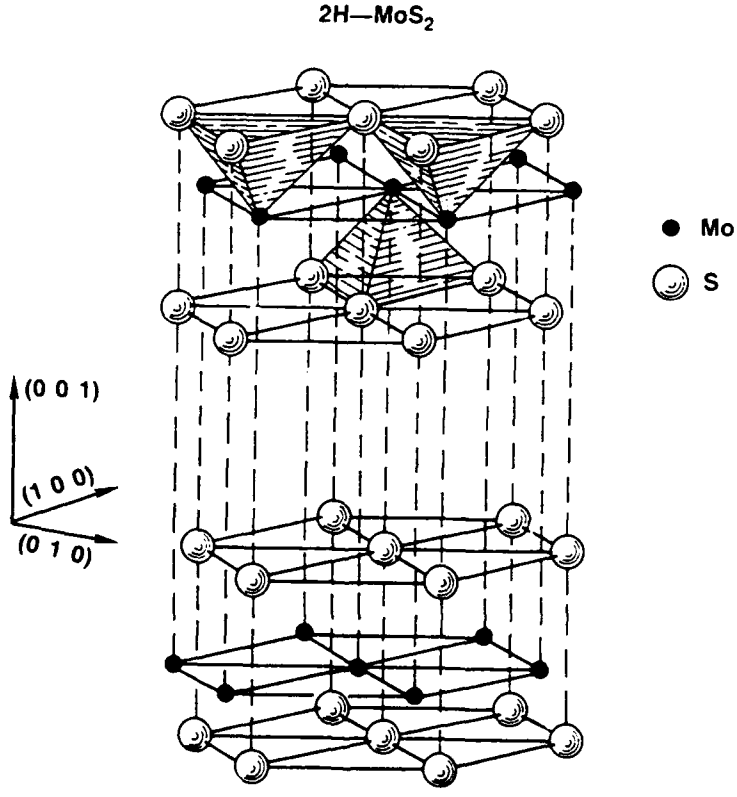

Figure 2. 2H-MoS_2 crystal structure indicating the layered-sandwich atomic arrangement and the crystallographic axes. The (0001) basal surfaces are present perpendicular to the (001) axis.

arrangements, crystal structure, and morphology [13-26]. Some recent theoretical interpretations of the surface science results have also proved extremely valuable [27,28].

1.3 TYPES OF SOLID LUBRICANTS

To be fair, we recount that there are numerous types of solid lubricants besides lamellar solids (layered materials), including soft metals, polymers, certain metal salts, reaction films, and diffusion coatings. Soft metals are useful for rolling contacts involving low contact loads; polymers for bushings, retainers, and sliding seals; and metal salts mostly for high-temperature applications. Reaction films and diffusion coatings are the results of surface modification procedures to provide, for example, oxide, nitride, or sulfide layers. These procedures are good for high-temperature conditions and also provide interlayers for other lubricating films. An excellent solid lubricant formulation, useful over a wide temperature range, combines the attributes of metal salts and soft metals [29]. All of these materials have important technological value and provide advantages for specific applications. But, few, if any, have been studied from the fundamental point of view, and certainly not to the extent that MoS_2 has, for the purpose of relating basic materials properties to application performance. In terms of surface science and the understanding it provides to tribological performance, the MoS_2 system offers a wealth of opportunities and challenges. We attempt to relate some of its unique and interesting properties in the following sections of this report.

2. MoS_2 SURFACE ELECTRONIC STRUCTURE

The surface geometric and electronic structures of solids are intimately related and, particularly in the case of the layered transition metal dichalcogenides (TMD), these properties control the surface lubricity and reactivity. The electron population of specific bonding, nonbonding, and/or antibonding orbitals centered on either Mo or S, along with the relative contributions of ionic and covalent bonding forces in MoS_2, determine surface electron density, bonding, and reactivity. In this section, we will focus on experimental and theoretical studies of the surface electronic structure of MoS_2 and examine the interplay among the geometric structure, electronic structure, and important tribological properties. The experimental work will focus on the use of surface-sensitive photoelectron spectroscopies (PES) employing both conventional and synchrotron sources to examine the valence band density of states, scanning tunneling microscopy (STM), and atomic force microscopy (AFM) to study atomic level surface geometry, electron density, and wear, and high-resolution electron energy loss spectroscopy (HREELS) to examine surface phonon dispersions. The theoretical studies range from relatively straightforward molecular orbital diagrams to extremely sophisticated *ab initio* calculations of the MoS_2 electronic structure.

2.1 SPECTROSCOPIC STUDIES

The relative ease of preparation of clean, well-ordered MoS_2 (0001) single-crystal surfaces by cleaving techniques has led to several experimental studies using surface-sensitive PES. Single crystals allow the study of well-characterized surfaces to permit comparison to polycrystalline lubricant films that typically have many defects. Historically, the first of these PES studies used conventional ultraviolet (UV) sources such as DC discharge lamps using H_2, He, and Ne gases as well as Mg and Al X-ray sources [30-32]. More recent work has employed synchrotron radiation to aid in spectral assignments [33-36]. These studies revealed a very rich valence band structure, with five well-resolved major peaks inviting detailed assignments. Typical valence band spectra obtained with synchrotron radiation are shown in Figure 3a with the spectral peaks resulting from electrons photoemitted from discrete energy levels in the solid. The well-resolved peaks and lack of surface states, which would typically appear above the valence band maximum in the band gap, in the Figure 3 data indicate that the MoS_2 surface is well ordered and contains few defects or dangling bonds (unsaturated bonds).

A binary compound presents some challenges for PES peak assignment, as electrons can be excited from valence orbitals centered on either atom. One must rely on a particular theoretical framework to understand the origins of the detected photoelectrons and to interpret PES data. Typically, those interested in electrical (e.g., semiconducting) properties of materials rely on band structure analyses [37], while those interested in chemical bonding and reactivity rely on a more localized molecular orbital (MO) theory interpretation. All PES data that we will discuss is angle integrated and, since we wish to focus on bonding and reactivity issues, it is more appropriate to use the MO interpretation of the MoS_2 valence band PES data.

The atomic origins of PES peaks can be determined by a widely used technique involving the variation of the incident photon energy and the detection of the resulting peak intensity changes. These changes can then be compared to those expected of the various atomic orbitals as deter-

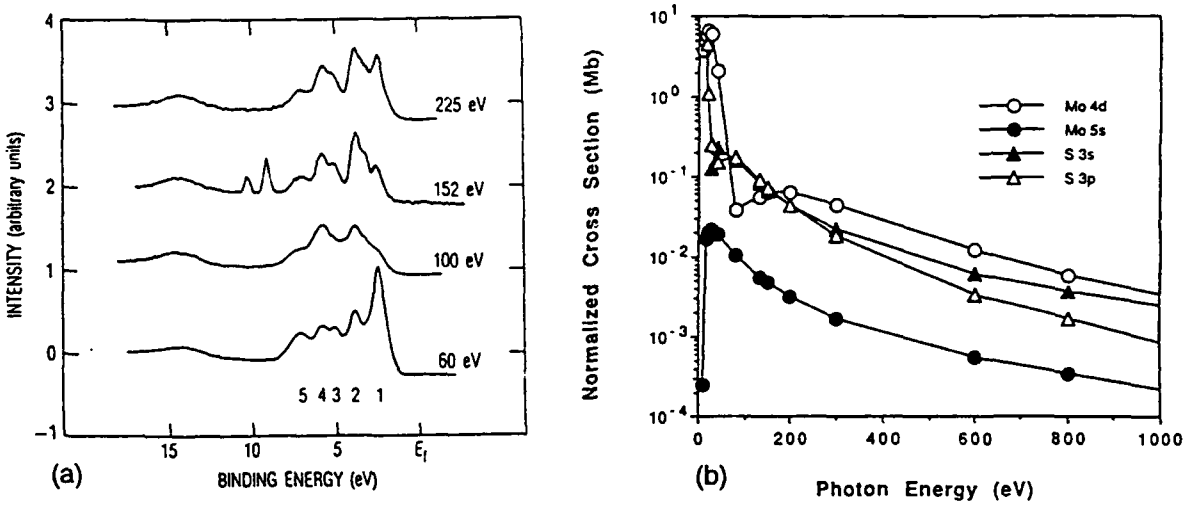

Figure 3. (a) MoS_2 variable photon energy valence band PES data obtained with synchrotron radiation. The incident photon energy for each spectrum is listed on the figure. Five main peaks are observed and labeled in the valence region. The peak near 15 eV is the S 3s, while the two additional sharp peaks in the 152 eV data result from second-order radiation causing photoemission from the S 2p core levels. (b) Theoretical atomic photoionization cross sections for the Mo 4d, 5s and S 3s, 3p subshells as a function of incident photon energy.

mined by theoretical atomic photoionization cross sections. By using linear combinations of atomic orbitals (LCAO) to form molecular orbitals (Eq. 1a), this approach can be used to assign the dominant atomic character in valence band PES peaks [38].

$$\Psi_{MO} = a\psi_1 + b\psi_2 + c\psi_3 + \ldots \quad (1a)$$

$$I(PES) \propto a^2\sigma_1 + b^2\sigma_2 + c^2\sigma_3 + \ldots \quad (1b)$$

In Eq. 1a, Ψ_{MO} is the wavefunction for the molecular orbital constructed from the linear combination of the atomic orbitals (ψ_1, ψ_2, ψ_3 ...) with the respective mixing coefficients (a, b, c,...). The intensity of the PES peak resulting from photoexcitation of an electron from this MO to the continuum can be approximated by Eq. 1b, where σ_1, σ_2, σ_3... are the photoionization cross sections of the respective atomic orbitals. This approach is only quantitatively valid at high photon energies (>200 eV) or when one atomic cross section dominates all others [39]; however, it is a good approximation even using lower energy excitation as in the following discussion.

The use of tunable synchrotron radiation has contributed greatly to detailed studies of the atomic orbital contributions to valence PES peaks through the use of variable photon energy PES. Figure 3b shows the theoretical photon energy dependence of the atomic photoionization cross sections of the important valence orbitals in MoS_2, the Mo 4d and 5s, and the S 3s and 3p [40]. Each atomic cross section has a distinct photon energy dependence, and differences are particularly evident at low photon energies (20 to 100 eV). Both Mo 4d and S 3p PES features should be very intense at low photon energies, but each cross section has a relative intensity minimum (called a Cooper minimum) at significantly different photon energies, approximately 35 eV for the S 3p and 90 eV for the Mo 4d. PES data obtained with various photon energies in this range have been used, in combination with Eq. 1b, to assign the dominant atomic orbital contributions to the occupied molecular orbitals in MoS_2, as shown in Figure 3. Increasing the photon energy from 60 to 100 eV causes a severe intensity decrease in the lowest binding energy peak 1 relative to all other valence band features. This behavior is due to the Mo 4d Cooper minimum and leads to the assignment of this peak as photoemission from a molecular orbital having dominantly Mo 4d character. The behavior of the remaining valence band features indicates that they are dominantly S 3p, but the energy splittings and differences in their photon energy-dependent intensity profiles signify that different additional atomic contributions exist in these orbitals. MO theory can be used to assign the spectral features, and the comparison of experiment and theory should produce a consistent picture of the MoS_2 electronic structure.

The chemical bonding forces in inorganic materials are generally believed to contain contributions from both ionic and covalent bonds. In general, MO diagrams for such materials are formulated by allowing the metal and ligand ions in their formal oxidation states to undergo covalent bonding interactions, essentially making the covalency a perturbation of the ionic energy levels. The trigonal prismatic local structure in 2H-MoS_2 creates a central Mo^{4+} ion bonded to six S^{2-} ions, while each sulfide ion is, in turn, bonded to three molybdenum ions (see Figure 2). Inorganic chemists normally focus on metal-centered complexes, and a qualitative MO diagram for MoS_2 in an appropriate cluster with D_{3h} symmetry, first reported by this research group [6,7], has been slightly modified and is given in Figure 4. This MO diagram predicts the existence of five different occupied valence levels, in agreement with the five major peaks in the PES data. With the formal oxidation state of Mo^{4+}, a d^2 electron configuration is expected, filling through the $2a_1'$ level, which is composed predominantly of the Mo $4d_{z^2}$ atomic orbital. All other occupied MOs are sulfur 3p-based and are split by bonding interactions with the unoccupied Mo $4d_{xz,yz}$ and $4d_{xy,x^2-y^2}$ ($1e''$ and $1e'$), 5s ($1a_1'$), and 5p ($1a_2''$ and $1e'$). The relative ordering of the S 3p-based MOs could conceivably be obtained from the effects of the Mo atomic orbital contributions to the PES peak intensity changes (se Eq. 1b). However, these changes can be quite subtle if the amount of covalent mixing is relatively small, or if the cross-section changes of the metal and ligand orbitals are not significantly different in the photon energy range used. An alternative means of exploring this problem further is available in resonant photoelectron spectroscopy.

Resonant PES is used to assign valence band features by exploiting intensity enhancements in particular peaks that occur when valence band data are obtained with photon energies that correspond to a core level absorption edge in the compound. The effect is particularly useful for transition metal compounds having unfilled nd orbitals at photon energies near the metal np absorption edge. The process of resonant intensity enhancement initiates when the metal core

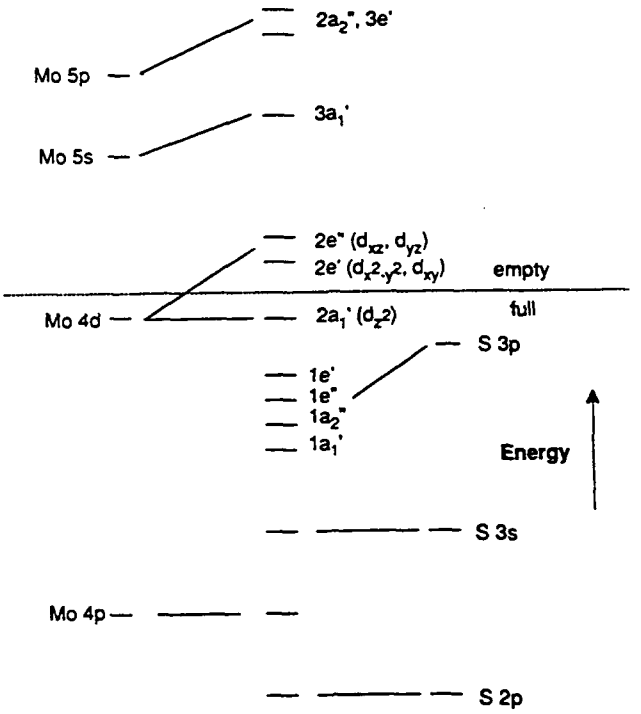

Figure 4. A molecular orbital diagram for 2H-MoS_2 constructed by considering an MoS_2 cluster with a central Mo^{4+} ion in a D_{3h} ligand field. The dotted line separates the empty and full energy levels, essentially marking the Fermi level in the material.

electron is excited to an empty metal valence level [41]. This excited state undergoes a super-Coster Kronig decay with one metal d-electron decaying to fill the core hole while a second metal d-electron is ejected as the photoelectron (Eq. 2a). The final electron configuration after this process is identical to the configuration after normal photoemission of a metal d-electron (Eq. 2b), resulting in an interference effect between the two pathways and, thus, enhancing any final state that has metal d-character (that is, any MO having d-orbital mixing).

$$np^6nd^x \rightarrow np^5nd^{x+1} \rightarrow np^6nd^{x-1} + e^- \quad (2a)$$

$$np^6nd^x \rightarrow np^6nd^{x-1} + e^- \quad (2b)$$

The resonant effect on the valence band spectrum of MoS_2 at the Mo 4p edge is shown in Figure 5. At the photon energy corresponding to the Mo 4p→4d transition (42 eV), the lowest binding energy feature (assigned as the Mo $4d_{z^2}$ based $2a_1'$) is enhanced by more than 300% when compared to its pre-resonance intensity [36].

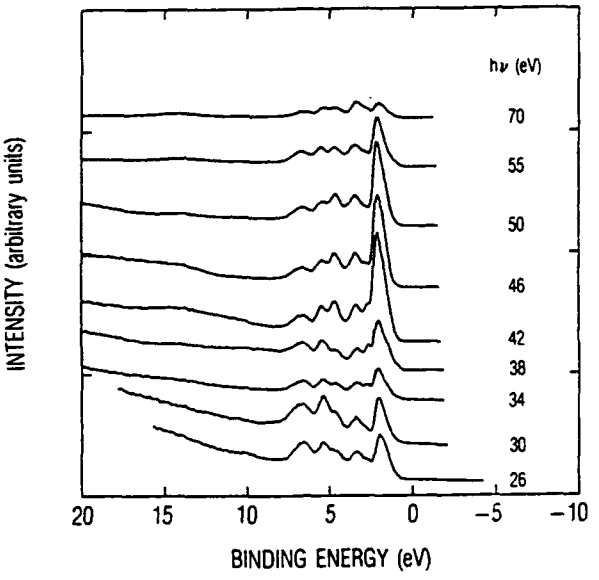

Figure 5. MoS_2 valence band PES obtained with photon energies that span the Mo 4p absorption edge. Resonant enhancement of peaks 1, 2, and 3 is clearly evident. (Reprinted with permission from authors of reference 36.)

The added utility of resonant PES in determining the MoS_2 electronic structure is the enhancement of particular S 3p-based PES features at the Mo 4p edge. Specifically, the two major lower binding energy S 3p-based PES peaks (peaks 2 and 3) are each enhanced by a factor of approximately 2 at the Mo 4p → 4d excitation energy, showing that these peaks contain significant Mo 4d character. By re-examining the MO diagram in Figure 4, these peaks can be assigned as photoexcitation from the $1e''$ and $1e'$ molecular orbitals formed through the covalent mixing of S 3p and the Mo $4d_{xz,yz}$ and $4d_{xy,x^2-y^2}$ orbitals, respectively. The relative ordering in the MO diagram is based on some chemical intuition where greater overlap would be expected for the e" orbitals based on the geometry of the MoS_2 system. The remaining major S 3p-based features at higher binding energies (peaks 4 and 5) experience only minor enhancement at these photon energies, leading to their assignments as the σ-bonding $1a_1'$ and $1a_2''$ levels, the latter of which is not allowed by symmetry to mix with Mo 4d orbitals. To summarize, PES has provided a rather complete picture of the valence band electronic structure of MoS_2. The challenge that will be addressed later is to relate this detailed electronic structure information to the important solid-lubricant tribological properties of film-substrate adhesion, lubricant film growth, and film lubricity (friction and wear properties).

2.2 ATOMIC LEVEL MICROSCOPY

Atomic-level microscopic techniques such as STM and AFM provide a means of studying the relationship between surface geometric and electronic structures of layered compounds [42]. The bonding geometry in the MoS_2 layers results in an 82° Mo-S-Mo bond angle. This geometry implies that the S-based orbitals described above are almost purely p-like (i.e., no hybridization with the S 3s or 3d) and that the three S 3p atomic orbitals on each S form σ-bonding molecular orbitals with three Mo ions. The resulting electronic structure has no p-π orbitals

extending above the sulfur plane, distinguishing the layered dichalcogenides from graphite. The orientation of the Mo $4d_{z}2$ orbital, with lobes centered among the three S atoms in the planes above and below and angular nodes aligned very closely with the Mo-S bond axes, limits its σ-overlap with S 3p-based a_1' ligand group orbital (the $3p_z$ orbitals along the bond axes), resulting in the essentially non-bonding highest occupied MO. These assumptions have been further studied with STM.

STM studies of the MoS_2 basal plane and other layered compounds have provided valuable information regarding their surface geometric and electronic structures. STM images of the MoS_2 (0001) surface revealed the expected hexagonal structure [22]. In addition, the images were obtained in air following cleavage of a single crystal, showing that well-ordered basal planes exist on MoS_2 after shearing upper layers (also observed in UHV with LEED) and that these surfaces are very stable and unreactive. STM images of MoS_2 were only obtained with a negative sample bias of at least -0.8 V, with the best images obtained at -1.5 V. The negative sample bias indicates that electrons were likely being removed from the Mo $4d_{z}2$ (highest occupied a_1' level) as the threshold for tunneling is close to the binding energy threshold for photoemission at the top edge of the valence band. Theoretical first principles calculations support this result by showing that electrons are most easily removed from the $d_{z}2$ orbital by a tunneling tip, and that while tunneling can occur from S species, the process is much less likely [28]. The presence of some Mo 4d electron density in the S-plane and the relative inaccessibility of the S 3p electrons should affect the interlayer bonding in MoS_2, an important consideration in determining the lubricity of this material.

Lieber and co-workers have performed several STM and AFM studies on MoS_2 and related compounds [25]. This work showed reproducible, periodic images of the MoS_2 basal planes using either technique, indicating that the electronic and geometric structures were consistent. Upon substitution of 10% Ni for Mo into the MoS_2 lattice, however, defects were apparent in the STM image, while the AFM image retained its defect-free, periodic structure, indicating an unperturbed basal plane geometric structure. The observation of defects with STM indicates a disruption of the electronic structure due to the Ni substitution and is consistent with the tunneling occurring from the metal d-orbitals in MoS_2. The nature of this perturbation is unknown since this is an unusual geometric configuration and oxidation state (assuming 4+) for Ni to adopt. In the 2+ oxidation state, Ni can adopt a trigonal prismatic geometry (as in NiAs), resulting in an unperturbed geometric structure but a vastly different local electronic structure, with a d^8 electron configuration and occupation of the $2e''$ and $2e'$ levels. Thus, the geometric orientation of the highest occupied Ni MO is significantly different than for Mo, as are the effective nuclear charge and the spatial extent of the d orbitals, all factors that should change electron tunneling properties.

The structural and electronic effects of substituting Se and Te for S in the MoS_2 lattice were also pursued [25]. In the Se substitution, a $MoS_{1.75}Se_{0.25}$ compound showed unperturbed STM and AFM images, with a small increase in the MoS_2 lattice parameters. The lack of obvious surface defects in both images indicated no significant disruption of either the electronic or geometric structures in the mixed compound. Alternatively, a $MoS_{1.75}Te_{0.25}$ compound showed significant variations in electronic and geometric structures. The AFM images showed localized protrusions due to the larger tellurium atoms, while the electronic images showed periodic, delocalized perturbations. The effects of these substitutions on the tribological performance of these materials has yet to be determined. One would expect the larger Se and Te species to be less electronegative

and more polarizable than S and, hence, change the nature of the interlayer forces. In addition, the protrusion of the Te atoms above the basal plane surface could significantly alter interlayer forces by creating a larger layer-layer spacing.

Lieber and co-workers [26] have also studied the layered $NbSe_2$ (0001) surface with AFM and have compared its structure, oxidation behavior, and wear rate to MoS_2. The two compounds have similar layered structures, but $NbSe_2$ has a different layer-layer registry, and the Nb^{4+} ion has a d^1 electron configuration. The work showed that $NbSe_2$ has more surface defects than a similarly prepared MoS_2 surface. The AFM study also showed that $NbSe_2$ was being worn approximately 5 times faster than MoS_2 by the instrument's scanning tip. Both compounds appeared to wear in a layer-by-layer fashion, but convincing evidence that MoS_2 was worn only along specific crystalline planes was obtained, while wear occurred over the entire scanned region in $NbSe_2$. Finally, the surface structures were examined after thermal oxidation in air, and the MoS_2 had far fewer and smaller surface defects than the $NbSe_2$, signaling greater reactivity for the d^1 compound. These results emphasize that the better tribological performance of MoS_2 can be studied down to the atomic level and is intimately related to both its geometric and electronic structures. These results are discussed further in following sections.

2.3 SURFACE VIBRATIONS

To obtain a better understanding of the nature of surface bonding properties, high-resolution electron energy loss spectroscopy (HREELS) has been used to map out the surface-phonon dispersions of MoS_2 and allow a comparison to bulk energies [16]. In addition, a knowledge of the surface vibration properties of MoS_2 is crucial in understanding the fundamentals of surface friction and energy dissipation for theoretical dynamic studies of solid lubrication. HREELS detects energy losses experienced by a monoenergetic beam of electrons upon interacting with a surface. The electrons lose (or gain) energy upon exciting (or de-exciting) surface vibration modes, either phonons in the substrate or stretching and bending modes of surface adsorbates. In addition, different selection rules for these momentum transfer events exist for electrons detected in the specular direction (dipole allowed) or off-specular (electron impact). These experiments detected a decrease in the energy of the surface phonons when compared to bulk values [43] as shown in Figure 6. The softening of these surface vibrational modes has been observed in another layered material, GaSe, and was attributed to lower force constants and increased polarizability of the surface Se atoms, leading to increased van der Waals attractions. The same phenomena are believed to exist in MoS_2, and LEED studies have observed a contraction between the first and second sandwich layers, indicating greater attraction between these layers than would occur if the lattice were continued with another MoS_2 layer [44]. The nature of the interlayer forces has always been assumed to be dominated by van der Waals forces that depend on the polarizability of the chalcogenide ion.

2.4 BONDING FORCES

The studies described above along with detailed electronic structure calculations are leading to an excellent understanding of the intralayer bonding properties of MoS_2. The consistency of experimental electronic structure studies with an MO description of the MoS_2 electronic structure indicates that significant Mo-S covalent bonding exists within a sandwich layer. In addition, binding energy shifts observed for both Mo 4d (+1.2 eV) and S 2p (-1.8 eV) core levels in MoS_2 relative

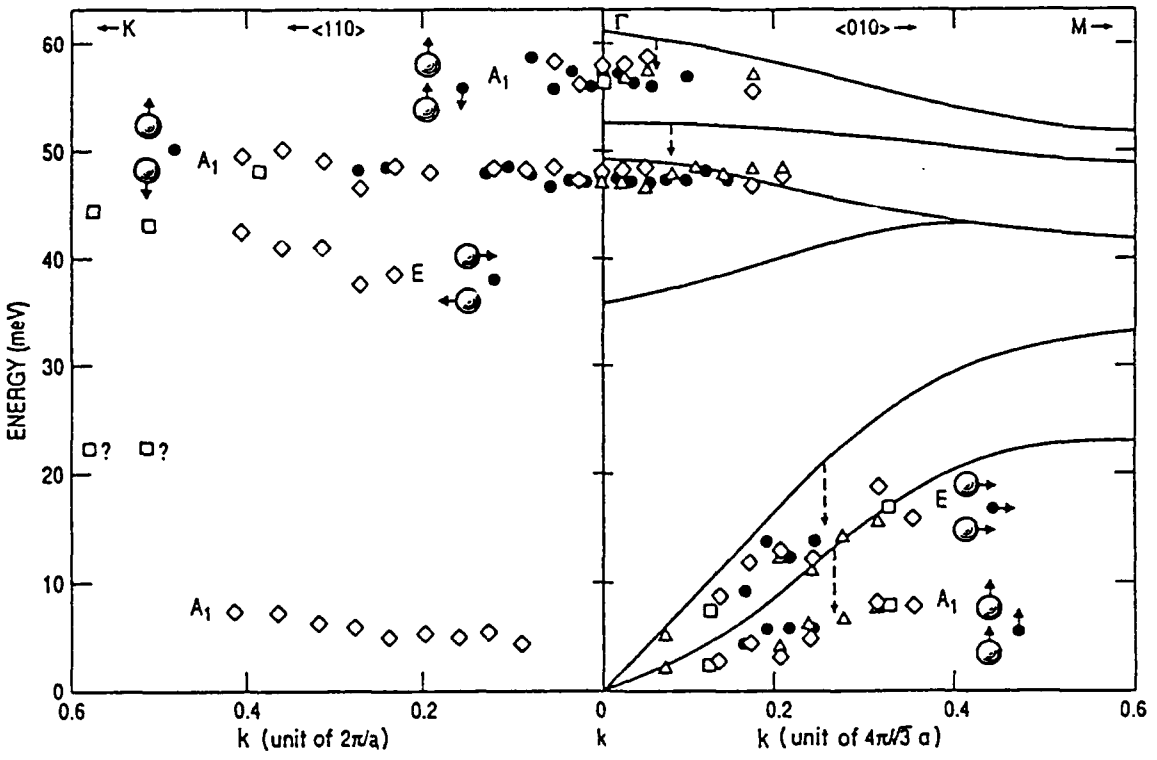

Figure 6. Surface phonon dispersion curves for MoS_2 along the (110) and (010) directions. Data are plotted with symbols and are compared to calculated bulk modes represented by solid lines (from Ref. 43). The various atomic displacements for each mode are represented next to the mode designation with ● representing Mo and ○ representing S in the layered structure. (Reprinted with permission from the author of reference 16.)

to elemental Mo and S indicate that some charge separation does exist on these species. The existence of charge separation implies that Coulomb attraction (ionic bonding) also contributes to the intralayer bonding in MoS_2. The relative contributions of the bonding forces, however, have not yet been established. For some first row transition metal oxides and chlorides, covalent bonding interactions are only believed to contribute 10 to 20% of the total energy stabilization, with Coulomb forces providing the rest [45]. The covalent contributions in MoS_2 are likely larger with the second row metal and softer sulfide ion, but the ionic forces cannot be ignored. Currently, detailed *ab initio* molecular orbital calculations are being conducted on Mo-S clusters of varying size to determine the extent of covalent mixing and the resulting distributions of electron densities. Currently, calculations performed on an Mo_7S_{26} cluster indicate that the Mo 4d-S 3p covalent mixing of fully coordinated Mo and S ranges from 20 to 40%, depending on the specific molecular orbital [46]. These calculations are aimed at reproducing the energy level splittings and orderings determined experimentally. Once final mixing coefficients have been obtained, the relative contributions of ionic and covalent bonding in these materials can be assessed. These issues are quite important to the understanding of the interlayer bonding forces in dichalcogenide compounds, which vary with both metal and chalcogen and control the lubricity of these materials.

The interlayer bonding forces present in MoS_2 and other similar lubricating dichalcogenides ($MoSe_2$, WX_2 compounds) have long been assumed to be predominately van der Waals interactions between the adjacent chalcogenide layers. It is clear that there are no covalent bonding interactions between layers, but several arguments point to Coulomb forces playing a role in interlayer bonding. For example, the registry of adjacent sandwich layers in the 2H-crystalline structure (Figure 2) is such that Mo atoms in one sandwich are located directly above and below S atoms in neighboring layers, maximizing the Coulomb attraction by minimizing the distance between oppositely charges species and maximizing the Mo—Mo separation. Also, MoS_2 has a very high melting point of 1185°C (it decomposes in air at 450°C), which is unusual for a compound thought to be held together by van der Waals forces. Although the strong intralayer bonding would preclude complete low-temperature melting, a fairly low-temperature, 2-dimensional "melting" transition would seem likely. In fact, all the TMDs have fairly high melting points, although structural phase transitions do occur. Finally, MoS_2 has shown the ability to intercalate and stabilize alkali metal ions between sandwich layers, showing that the sulfur species are capable of ionic bonding [47]. Thus, while short-range van der Waals attractions ($\propto r^{-6}$, where r is the distance between interacting species) between neighboring sulfur basal plane layers take place, longer-ranged Coulomb forces ($\propto r^{-1}$) almost certainly play a role in interlayer bonding, despite the fact that the nearest layer-layer interacting species are the sulfide ions of adjacent basal planes, resulting in a repulsive force. A Madelung-type calculation on the layered structure would be very instructive in the determination of the role of Coulomb forces once accurate charge densities have been determined. An understanding of these forces will eventually allow molecular dynamics calculations of MoS_2 planes moving relative to one another to enhance our understanding of solid lubrication.

Many different transition metals form layered dichalcogenide structures, including Ti, Zr, Hf, V, Nb, Ta, Mo, and W. This list provides some interesting insights into these materials. First, the metal must have at least four valence electrons to achieve the 4+ formal oxidation state. Second, only atoms early in the transition metal series are able to form these compounds. Third, of all of the layered compounds, only the dichalcogenides of Mo and W have found widespread use as lubricants. The keys to understanding these observations exist in the electronic structure of the layered materials.

The fact that the layered structures exist, and are indeed the MoS_2 structures found in nature (molybdenite), indicates that they are the lowest energy geometric structures for the S and Se dichalcogenides to adopt; no oxides adopt these structures. Other possible structures observed for transition metal compounds with this stoichiometry (including oxides of these same metals) are rutile (and other TiO_2 structures), fluorite, and several other structures where the metal is octahedrally coordinated (e.g., pyrite). Why are the different layered structures preferred? One possible explanation is that steric and/or Coulombic interactions with the larger chalcogens cause the layered structure to be the lowest energy structure. A second explanation may be in the d-orbital configuration and electron occupation present in these materials.

The different layered dichalcogenides actually have different local bonding geometries and stacking registries. The group 6B metals (Mo and W) form the trigonal prismatic structure with D_{3h} local geometry about the d^2 metal ion. The group 4B metals (d^0) form only O_h geometries about the metal. The group 5B metals (d^1) have varying structures: NbS_2, $NbSe_2$, and $TaSe_2$ are trigonal prismatic; VS_2 and VSe_2 are octahedral; and TaS_2 forms both structures. Hoffmann and

co-workers [48,49] have discussed this in detail, focusing on high symmetry points in the electronic band structures and ligand energy level stabilization, concluding that octahedral geometries are favored for all electron populations except for d^1 and d^2. A simple MO discussion of d-electron orbital filling in the different geometries can also reach this conclusion if the t_{2g} orbital set in O_h geometries is considered to have more π^* character than the $2a_1'$ orbital in D_{3h}. This assumption is reasonable because the d_{z^2} orbital in the trigonal prismatic geometry is aligned at an angle with respect to the ligand a_1' orbitals (p_z), which are along the M-L bond axes. This orientation does not allow typical π-overlap to occur effectively (the lack of σ-bonding for the d_{z^2} orbital has already been discussed). Alternatively, the t_{2g} d-orbital set in O_h compounds is composed of the $d_{xy,xz,yz}$ orbitals, which are perfectly arranged for effective π-overlap with the ligand $p_{x,y}$ orbitals. Using these considerations, the relative d-orbital manifold splittings for the two geometries are shown in Scheme I.

Scheme I

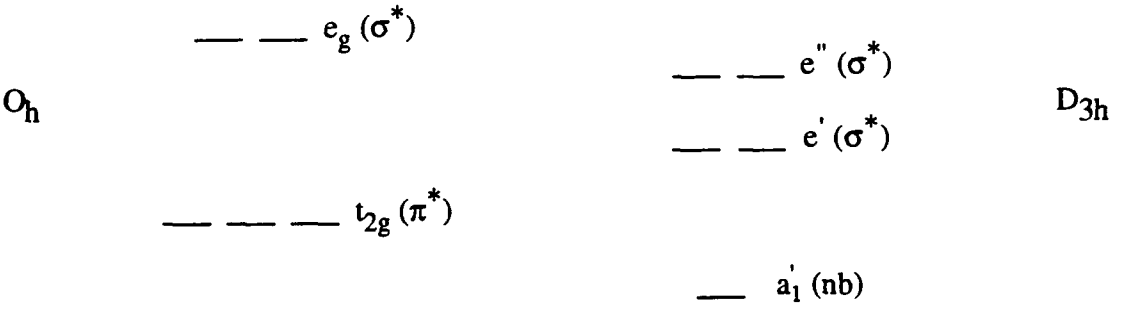

The filling of the d-based molecular orbitals should play a significant role in determining the most stable geometric structures. For d^2 compounds, the trigonal prismatic geometry is favored by filling the nonbonding a_1' orbital rather than the antibonding t_{2g} in O_h.[1] Trigonal prismatic geometries are very rare for d^3 or higher occupation compounds as more d-electrons would begin to fill the σ^* (e' and e") levels, which are clearly destabilized to higher energy than the π^* t_{2g} set for octahedral materials. As a result, octahedral or other (e.g., tetrahedral) geometries are preferred with increasing d-orbital population. Huisman et al. have performed calculations to address the relative stabilities of the trigonal prismatic and octahedral structures, although in their model, greater covalent mixing for the second and third row transition metal compounds explains their preference for the trigonal prismatic structure [50].

The existence of some trigonal prismatic structures for the d^1 group 5B dichalcogenides is also explained by this electron occupation model, but the stabilization effect provided by the D_{3h} symmetry is lessened due to the single electron occupation. The presence of some octahedral TMDs having d^1 electron configurations indicates that the energy differences between the two structures are not great. The group 5B dichalcogenides may also have some metal-metal interlayer bonding interactions using the half-occupied d_{z^2} orbitals. This bonding interaction causes the metal atoms in adjacent sandwich layers to align, increases three-dimensional conductivity,

[1] This argument ignores the possible contribution of exchange interactions that would tend to favor the unpaired electrons in the O_h t_{2g} orbitals.

decreases the lubricity of these materials relative to Mo and W dichalcogenides, and adds additional stability to the structure. The intercalation of coinage and alkali metals into the d^1 compounds significantly alters their geometric, electronic, and tribological properties by donating an electron to the a_1' level, essentially creating a d^2 metal ion. The result is a change in the crystalline registry, a decrease in conductivity, and increased lubricity. In short, the material becomes much more like d^2 MoS_2.

Since the group 4B metals have no available d-electrons to fill the d_{z^2} level, one must conclude that the exclusively octahedral geometry adopted by these compounds provides the more stable structure when only steric and/or Coulombic factors are considered. Alternatively, a combination of steric/electrostatic and electronic structure factors determine the geometric structures of the other compounds. Indeed, an octahedral arrangement of the chalcogenide ions creates a staggered intralayer AB close-packing that would intuitively have lower energy than the AA layer stacking in the trigonal prism. Madelung calculations of the different structures would appear to support this notion [49]. Kertesz and Hoffmann argue that octahedral geometries of d^0 configurations are also more stable electronically, but the differences in the two geometries are quite small [48].

2.5 ELECTRONIC STRUCTURE AND LUBRICITY

The interplay between the electronic structure and lubricity for the MoS_2-like layered dichalcogenides should now be apparent. Weak interlayer bonding interactions result in low shear strength parallel to the (0001) basal planes. The interlayer bonding interactions are potentially controlled by covalent, ionic, and van der Waals interactions. A species having covalent interlayer bonding interactions (such as $NbSe_2$) is not as good a candidate lubricant as one without such interactions. It should be noted that these covalent Nb-Nb bonds are probably fairly weak due to the large metal-metal separation, but the difference in structure from MoS_2 where the Mo ions are aligned with sulfides shows the interaction to be important. Also, the work of Lieber et al. shows that $NbSe_2$ basal planes wear faster than MoS_2 at the atomic level and are more reactive [26]. These properties result from the enhanced bonding capabilities of the Nb atom in $NbSe_2$ due to the singly occupied $2a_1'$ level, allowing adhesion of the surface to the scanning tip and more facile reactivity. Alternatively, the d^0 titanium dichalcogenides are too brittle to perform effectively as lubricants, showing that the greater ionic character caused by the more electropositive metal is reducing the materials' lubricities. The balance between intralayer ionic and covalent bonding in MoS_2 must contribute to a balance in the interlayer Coulombic and van der Waals interactions, leading to a material with very low shear strength in two dimensions.

The understanding of electronic structure and its role in tribology might allow these materials to be tailored to suit specific lubrication needs. For example, the semiconducting MoS_2 is often used in compacts to provide a lubricating and conductive interface for moving electrical contacts. The substitution of electron-deficient metal ions (e.g., Nb) into the MoS_2 lattice would likely enhance the conductivity without greatly affecting lubricity. (Doping for electronic purposes usually requires a very small number of atoms that would likely have little effect on the lubricating ability of the entire compound [51].) Furthermore, since interlayer forces are affected by both ionic and van der Waals forces, replacement of some of the sulfide ions with ions having significantly different electronegativities and polarizabilities should change interlayer bonding and affect the friction and wear of lubricated surfaces.

2.6 ELECTRONIC STRUCTURE AND SURFACE REACTIVITY

The geometric and electronic structures of MoS_2 provide for very interesting surface reactivity. In general, the (0001) basal planes are very inert toward adsorption of contaminants and oxidation. This occurs because the highest occupied MO is the full $2a_1'$ ($4d_{z^2}$), which is relatively inaccessible through the upper sulfur layer of the surface sandwich. Thus, even though higher oxidation states of Mo are quite stable, the basal plane of MoS_2 is difficult to oxidize. In addition, the occupied S-based molecular orbitals are much more energetically stabilized than the $4d_{z^2}$ level, as well as being directed primarily toward the central Mo ion as bonding orbitals, requiring more energy to remove electrons from the surface. This is a very important result to consider for the storage of MoS_2 lubricants, where one would conceivably prefer a lubricating film to have maximum basal plane exposure to a potentially reactive environment. This orientation also maximizes the lubricity of the material because the inert (0001) planes provide the low shear surface for lubrication. The unoccupied Mo-based antibonding orbitals (e' and e'') are not readily accessible through the basal plane but are exposed at edge plane sites, making the chemical reduction of MoS_2 unlikely at the basal plane. The addition of electrons into these levels should promote the decomposition of MoS_2, as will be discussed in the following section.

Several studies have shown that surface defects and MoS_2 edge sites are much more reactive than pristine (0001) planes. In particular, such defects have been shown to be sites for the initiation of oxidation [52,53] and of gold decoration [54]. Intuitively, one would also expect such sites to be nucleation sites for MoS_2 film adhesion and oxidation for lubricating films. Later in this report, the nucleation and growth of sputter-deposited MoS_2 films will be discussed in terms of edge plane growth versus basal plane growth.

A final possibility to address is the alteration of the adhesion of an MoS_2-based lubricant film to a surface by incorporating dopant materials into the first film layers. One could presumably change the reactivity of the basal plane by substituting for S with an electron-poor species, such as P or As, which can form bonds with metallic surfaces by removing electrons to complete its subshell occupation. Of course, such a dopant would significantly alter the local electronic structure in as yet undetermined ways. Experiments are planned in the near future to determine the feasibility of such ideas.

3. MoS_2 SURFACE REACTIVITY

3.1 CORE LEVEL PES WITH SYNCHROTRON RADIATION

The low-shear strength of the (0001) basal plane of MoS_2 allows this material to act as a lubricant. Ideally, it is preferable for the (0001) planes of the crystallites in a film deposited to act as a lubricant to be oriented along the direction of motion on the surfaces being lubricated, i.e., parallel to the surface plane. Defect-free (0001) planes, however, contain no dangling bonds, hindering the MoS_2 basal plane's ability to form strong substrate bonds. Studies of the (0001) surface reactivity have been pursued with hopes of developing a strategy for improving surface adhesion (bonding) without compromising the lubricating properties of MoS_2. A significant portion of this work has used the surface-sensitive nature of PES to follow the surface reactions occurring during ion bombardment of the MoS_2 basal plane and also to study the chemical reactions occurring between the (0001) surface and selected metals.

Core level (as distinguished from valence level) photoelectron spectroscopy has been used for many years to study the oxidation states and surface reactivities of materials. This work originated with the notion of the chemical shift of atomic core levels obtained with XPS [55]. Simply stated, the measured kinetic energy of an electron photoemitted from an atomic core level depends on the oxidation state and/or bonding environment of the atom. The kinetic energy is related to the binding energy of the electron in the solid, and electrons emitted from higher oxidation state species generally appear at higher binding energies than those emitted from the same core level of a lower oxidation state species. Alternatively, an atom covalently bonded to a more electronegative atom will experience a decrease in electron density, and the photoemitted electrons will again appear at higher binding energy (lower kinetic energy) than electrons emitted from an atom bonded to less electronegative neighbors. By carefully obtaining and analyzing core level data, a great deal can be learned about surface bonding and reactivity.

Two factors that greatly influence the utility of PES to study surface reactivity are its surface sensitivity and the energy resolution of the technique. The escape depth (scattering length) of an electron photoemitted from a solid depends strongly on its kinetic energy [56]. A limitation of using X-ray excitation (for XPS) to study core levels in solids is that the kinetic energies of the detected electrons are often large enough to produce photoelectrons from fairly deep into the bulk of the material (as deep as 5 to 10 nm), lessening the relative contribution of electrons emitted from the uppermost atomic layer to the data. In addition, the energy resolution of X-ray sources is often on the order of 1 eV, which limits the chemical shift detail that can be obtained from such work. The advent of synchrotron radiation to study surface chemistry with PES has solved both of these problems. The tunable nature of synchrotron radiation allows the kinetic energy to be altered to achieve maximum surface sensitivity. Also, core levels of different surface species having different binding energies can be excited with appropriate photon energies to produce photoelectrons having the same kinetic energies, thus ensuring that the different chemical species being studied are at the same depth in the sample. Finally, many synchrotron monochromators are capable of providing a significantly narrower line width than is available with conventional X-ray anodes, permitting higher resolution data that can provide more detailed chemical bonding information.

3.2 ION BOMBARDMENT WORK

One area of MoS_2 surface chemical reactivity that has been studied is the effect of noble ion bombardment of the (0001) surface. This work has relevance for two important reasons: (1) most MoS_2 deposition techniques use inert ions to sputter deposit films on substrates; and (2) the bombardment of the inert basal plane was thought to be a possible route to increase the reactivity and enhance the adhesion of this crystal face to a surface.

Noble ion (Ne^+, Ar^+) bombardment of (0001) MoS_2 has been studied using relatively low-resolution XPS [57,58] and Auger electron spectroscopy [59,60]. Every such study (with ion energies ranging from 300 eV to 10 keV) has detected a decrease in the S:Mo surface concentration ratio, indicating that S is preferentially removed from the surface. Presumably, this would create surface defects and increase the reactivity of the (0001) surface. The XPS work detected shifts of both the Mo 3d and S 2p core levels to lower binding energies, but could not distinguish new features related to the formation of new surface species.

Higher resolution, more surface sensitive PES experiments were needed to determine the detailed chemical changes occurring with ion bombardment. Such a study was performed using Ne^+ bombardment and synchrotron radiation to tune the surface sensitivity of the technique [61]. In these data, the Mo 3d spectra were obtained with 300 eV photons while the S 2p spectra were obtained with 230 eV photons. These photons energies produced photoelectrons from the two core levels with virtually the same kinetic energies (approximately 65 eV), and hence the same effective escape depth from the surface.

The effects of increasing doses of 1 keV Ne^+ ions on the Mo $3d_{5/2,3/2}$ and S $2p_{3/2,1/2}$ doublets are shown in Figure 7. Also included on the figure are the best computer fits to the data obtained with Voigt functions and a Shirley background [62]. In short, increased ion bombardment leads to the development of new surface species with PES peaks at lower binding energy in the case of Mo and at higher binding energies for S, relative to the MoS_2 peaks. The chemical shift of the reduced Mo species is not as great as expected for metallic Mo, but larger than expected for other known oxidation states of Mo. A possible reason for this intermediate binding energy is that the Mo exists in highly dispersed, small clusters or islands of metal-like atoms. Higher than expected binding energies for highly dispersed metal atoms have been observed on many surfaces, with the high binding energies explained by decreased extra-atomic relaxation capabilities of the ionized species (a final-state effect [63]).

The changes observed in the S 2p data are more subtle than observed for the Mo 3d. In general, the formation of small features at higher binding energy than the MoS_2 sulfide ion peaks is observed, indicating that a small number of surface sulfide ions have been oxidized. The chemical shift is not large enough to indicate the existence of elemental sulfur, but the existence of charged $(S\text{-}S)^{x-}$ surface species [64] was hypothesized. In general, the small magnitude of change observed in the S peaks relative to the extensive changes observed in the Mo peaks is consistent with the loss of many of the surface S species (by preferential sputtering) that were previously bonded to the Mo species that have formed the metallic islands upon ion bombardment.

The valence band PES spectrum was also followed with ion bombardment and showed a general decrease in the resolution of the peaks discussed in Section 2 with increased bombardment. In

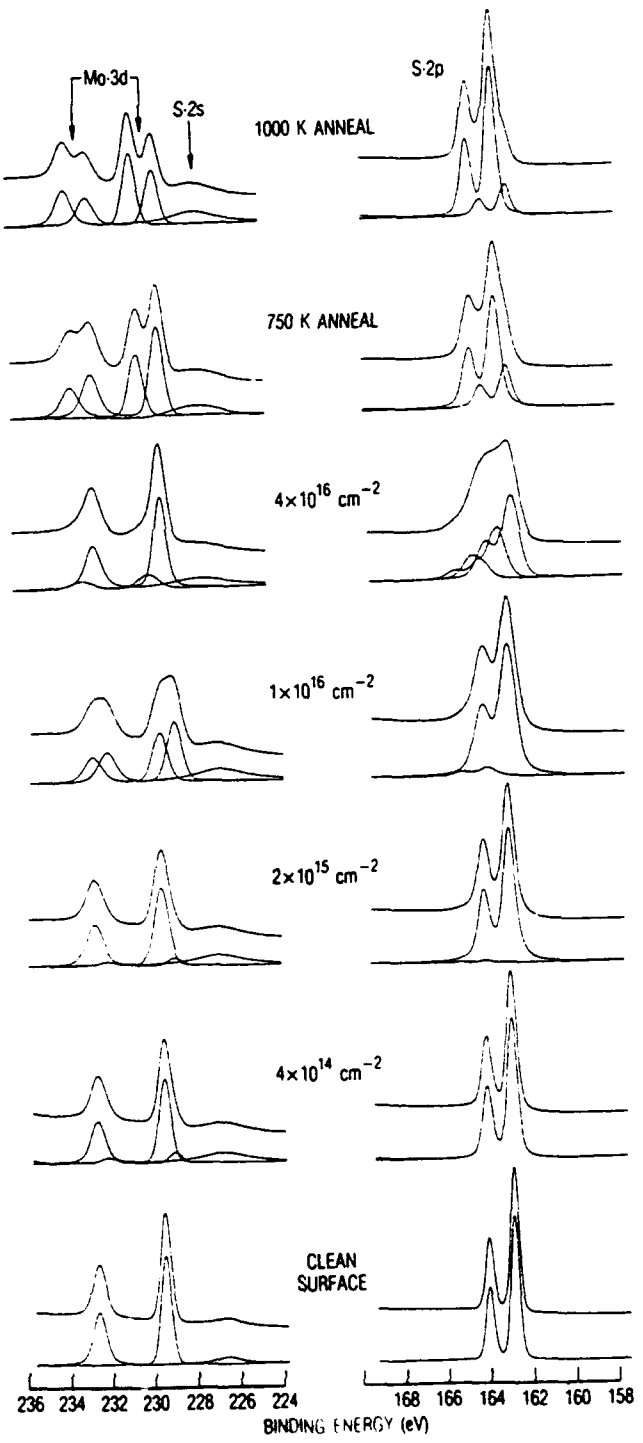

Figure 7. The Mo 3d (left) and S 2p core levels as a function of Ne^+ ion bombardment or annealing as listed on the figure. These data were obtained with synchrotron radiation as detailed in the text. The S 2s level is also evident in the Mo spectral data. The doublet structure observed for all Mo 3d and S 2p data arises due to the spin-orbit interaction present in the ionized final state. (Reprinted with permission from author of reference 62.)

addition, more electron density was observed near the Fermi level of the material, consistent with the formation of a more metallic surface. Upon annealing to 1000K, much of the order in the valence band data is restored, indicating that some of the surface damage can be healed. However, the core levels following this anneal still show the existence of a significant amount of metallic Mo and a small amount of non-sulfide sulfur, indicating surface disorder (see Figure 7).

This detailed study of the chemical composition of the (0001) MoS_2 surface as a function of ion bombardment has shown that the chemical reactivity of the surface most certainly can be changed. One would expect an ion bombarded surface to be more reactive than a pristine basal plane due to the presence of metallic-like Mo islands, many sulfur defects, and surface species in other chemical states. The creation of a S vacancy would effectively leave 2 electrons to populate either localized Mo 4d orbitals at the defect site or the delocalized MoS_2 conduction band. If the electrons remain localized (consistent with the detection of reduced Mo in PES), then a highly reactive defect that could be easily oxidized should result. This type of defect would probably interact strongly with electron-accepting species, but would not likely enhance the adhesion of MoS_2 to a metallic surface. Alternatively, the removal of a sulfur atom from the basal plane would allow greater access to the Mo ion and, if the electrons become delocalized into the conduction band, perhaps facilitate bonding with electron-rich species.[2] In either case, the excess electrons would enter antibonding orbitals and tend to destabilize the MoS_2 structure to some degree unless they enter into a chemical bond. Whether this behavior can be used to enhance the adhesion of a lubricating MoS_2 film to a particular substrate is unknown, but it almost certainly plays a role in MoS_2 film growth by physical vapor deposition techniques, which will be discussed in detail in Section 4. Specifically, the preferential sputtering of S from a deposition target would appear to create a sulfur-rich plasma in many sputtering techniques. Also, the use of ion-beam-assisted deposition to densify films likely alters the chemical make-up of the MoS_2, making it sulfur-poor.

3.3 METAL-MoS_2 REACTIVITY

Core level PES studies similar to those just discussed have been performed following evaporation of various metals onto the (0001) MoS_2 surface. These studies are important for understanding both MoS_2-substrate interactions and the chemistry occurring in the growth of MoS_2 films containing metal dopants. We will discuss the results for metals that can have significance for MoS_2 interactions with steel surfaces. Several studies conducted with other metals showed that very little reactivity of most metals with the basal plane is detected by XPS [65]. The high-resolution, very surface-sensitive studies discussed below indicate that while bulk chemical reactions of the MoS_2 basal plane with metals are rare, significant interfacial chemistry does occur.

The many studies of metal/MoS_2 reactivity have demonstrated that the reaction to form metallic Mo and the deposited metal sulfide must have a negative or slightly positive free energy (ΔG_{rxn}) to proceed at room temperature. However, only a few metals (Mg, Ti, and Mn) meeting this condition react extensively with MoS_2 [45]. Metals that are particularly important for steel surface adhesion (e.g., Fe, Cr, Ni) have minimal bulk reactivity to form the new metal sulfide. It is necessary to investigate the interfacial reactivity of such metals in order to determine if chemical

[2] As noted earlier, such defect sites have been shown to be the initial sites of surface oxidation and of gold decoration, showing a tendency to interact with electron accepting and relatively inert species.

bonds between MoS_2 and these important substrate materials can be formed. We have chosen to examine a reactive metal (Mn) along with Fe and Cr, the most important metals involved in steel surface chemistry.

3.3.1 Mn/MoS_2 - A Reactive Interface

The Mo 3d and S 2p core levels from a (0001) MoS_2 surface as a function of Mn deposition are shown in Figure 8 [66]. Once again, the photon energies have been tuned to generate photoelectrons with similar kinetic energies. These data clearly show that a new, lower binding energy S species forms at coverages equivalent to 22 Å of Mn,[3] along with a small amount of metallic Mo. At higher coverages, the reaction continues, and when enough Mn has been deposited to successfully cover the entire sampling region (the equivalent of 58 Å thickness), no Mo signal is observed while S peaks with binding energies expected for MnS are present. The Mn 3p peaks obtained, following these same depositions show a broad feature whose maximum is centered at the binding energy of metallic Mn. This feature is broadened to higher binding energy, indicating the presence of higher oxidation state Mn compounds (presumably MnS). When the 58 Å Mn/MoS_2 surface is heated to 770K, wholesale reaction of all of the metallic Mn to MnS is observed. Simultaneously, the molybdenum signal reappears at a binding energy indicative of metallic Mo. These PES results are entirely consistent with the bulk reaction:

$$Mn + \tfrac{1}{2}MoS_2 \rightarrow MnS + \tfrac{1}{2}Mo\,, \qquad (3)$$

which has a ΔG_{rxn} of -25.2 kcal/mole. Some room-temperature reaction occurs, but the higher temperature drives the reaction to completion, overcoming kinetic barriers that may be the result of the highly stable MoS_2 (0001) surface. This large-scale reaction is not necessarily desirable to enhance MoS_2 adhesion to a metallic substrate because the formation of an entirely new compound may prove highly detrimental to the bonding of MoS_2 to the metal as well as signal the possible breakdown of the lubricant by the substrate. For example, Spalvins observed that the formation of interfacial copper sulfides when MoS_2 was deposited on a copper substrate led to significantly decreased adhesion of the film [67].

[3] The coverages indicated result from thickness monitors used to calibrate evaporation rates and assume a uniform, three-dimensional film growth. In reality, the measurement indicates that the total amount of deposited material and the film structure is defined by surface reactions.

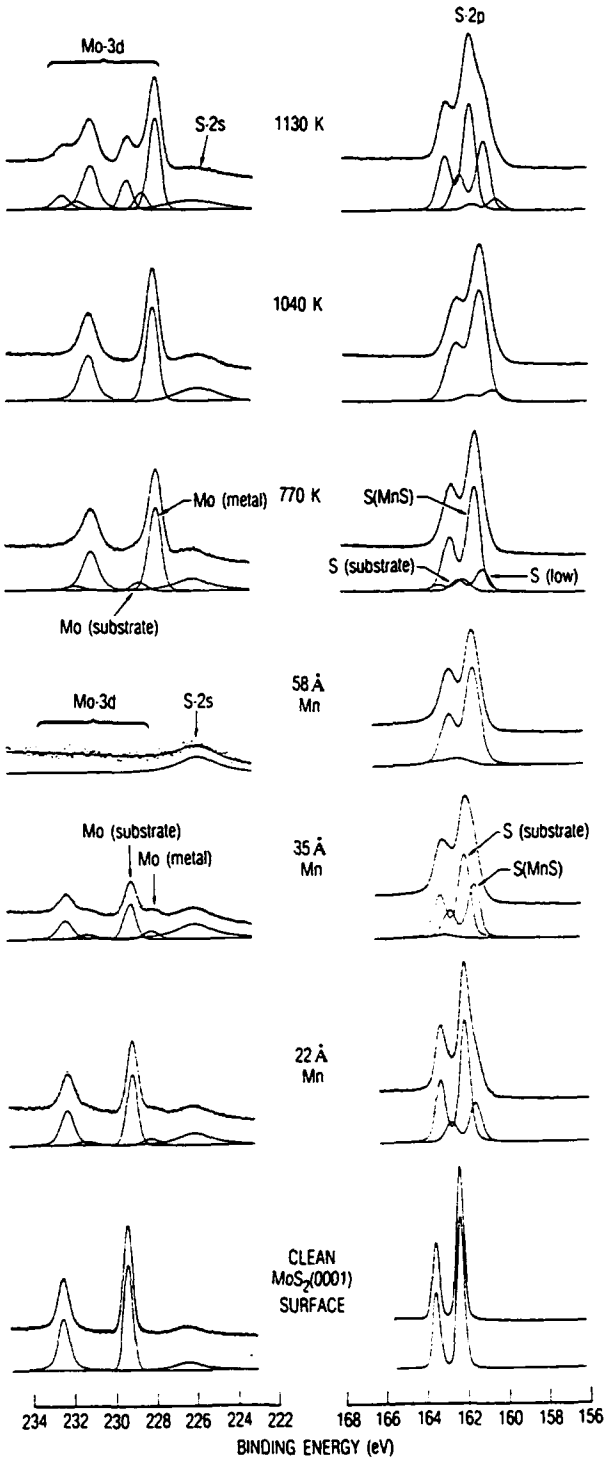

Figure 8. The Mo 3d (left) and S 2p core levels of MoS_2 obtained as a function of Mn-metal deposition and subsequent high-temperature anneals. Various chemical species are identified on the spectra. (Reprinted with permission from the authors of reference 66.)

3.3.2 Fe/MoS_2 - Interfacial Chemistry

The interaction of MoS_2 with Fe is potentially the most important reaction controlling the adhesion of this lubricant to steel surfaces. Compared with the extensive reaction with Mn discussed above, the reactions of Fe and MoS_2 to form bulk iron sulfides are not thermodynamically favorable.

$$Fe + \tfrac{1}{2}MoS_2 \rightarrow FeS + \tfrac{1}{2}Mo \qquad \Delta G_{rxn} = +3.2 \text{ kcal/mole} \qquad (4a)$$

$$Fe + MoS_2 \rightarrow FeS_2 + Mo \Delta G_{rxn} = +14.1 \text{ kcal/mole} \qquad (4b)$$

The Mo 3d and S 2p PES core levels are shown in Figure 9 as a function of Fe coverage on a (0001) MoS_2 surface [68]. Unlike the Mn/MoS_2 interface, there is no large-scale formation of new compounds with increasing iron overlayer coverage, although some small changes do occur. The Mo 3d peaks virtually disappear when 10 Å of Fe has been evaporated onto the surface, showing that iron forms a more uniform, continuous overlayer than Mn. A significant amount of S associated with the Fe overlayer is detected, and computer fits to the data indicate the presence of two predominant species, an iron sulfide phase and S adsorbed onto metallic iron. Annealing the Fe/MoS_2 surface does not promote the formation of more iron sulfide, but rather uncovers the MoS_2 substrate as the Fe overlayer coalesces into three-dimensional features. Significant amounts of metallic Mo are only observed at very high temperatures (1200K).

The iron overlayer is obviously much less reactive on MoS_2 than the Mn layer discussed above. However, some interfacial chemistry does occur as evidenced by the production of a small amount of an iron sulfide and the migration of some sulfur to the top of the iron overlayer to form an adsorbed species. It is possible that this limited interfacial reactivity may promote better adhesion of MoS_2 films to steels than a highly reactive interface. The limited reactivity appears to allow for the formation of Fe-S bonds without the large-scale formation of bulk iron sulfides. It is apparent that an undesirable breakdown of an MoS_2 lubricant by reaction with an iron-containing substrate should not occur. However, this limited reactivity may not provide adequate film/steel adhesion to promote long endurance during wear. These are important points in considering the potential success of using these materials as solid lubricants on steels. Zabinski and Tatarchuk have detected the formation of a Chevrel phase $FeMo_2S_4$ using Conversion Electron Mossbauer Spectroscopy at the interface of a 25 Å thick film on MoS_2 after heating to 923K, indicative of the formation of a distinct new phase [69]. These compounds were not evident in the PES results but may exist interfacially between the metal islands and the MoS_2 substrates. However, although reactivity at such high temperatures may produce the most thermodynamically stable species, most steels should not be subjected to these temperatures either during or after coating with MoS_2, and the existence of metastable phases at lower temperatures cannot be precluded.

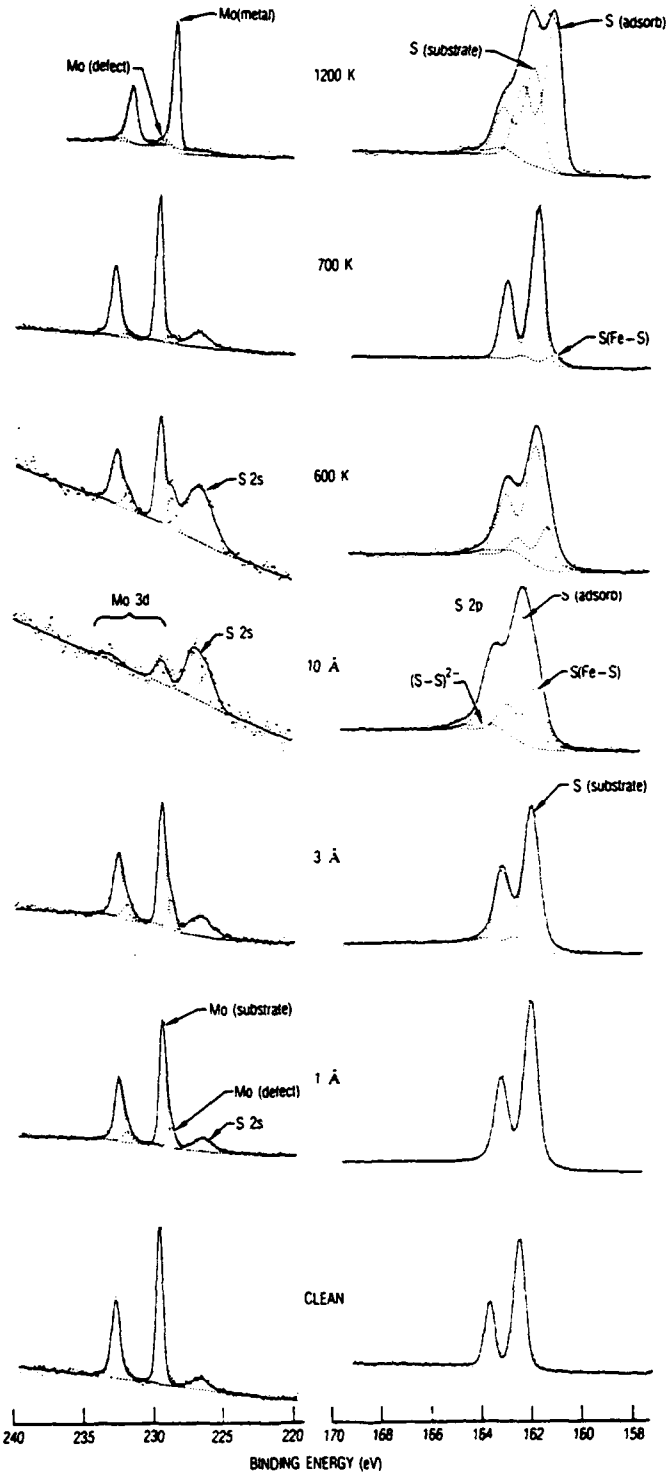

Figure 9. The Mo 3d (left) and S 2p core levels of MoS_2 obtained as a function of Fe-metal deposition and high-temperature anneals. Note the lack of significant metallic Mo in contrast to that observed in the Mn/MoS_2 data presented in Figure 6. (Reprinted with permission from authors of reference 68.)

3.3.3 Cr/MoS_2 - Intermediate Reactivity

The presence of chromium in varying amounts in stainless steels makes its reaction with MoS_2 important. This is particularly true because the Cr tends to segregate to the steel surface region to form a corrosion-resistant chromium oxide layer. This same segregation may cause Cr to interact with MoS_2 at its interface with stainless steels, possibly leading to beneficial or deleterious chemical processes. In keeping with the above discussions, the reaction of metallic Cr with MoS_2 is slightly favored thermodynamically.

$$Cr + \tfrac{1}{2}MoS_2 \rightarrow CrS + \tfrac{1}{2}Mo \qquad \Delta G_{rxn} = -10.1 \text{ kcal/mole} \qquad (5)$$

Figure 10 shows the Mo 3d and S 2p core levels as a function of Cr coverage [70]. The Mo 3d peaks show the emergence of a limited amount of metallic Mo when Cr is deposited. All of the Mo PES peaks have very low intensity when 16 Å of Cr is present on the surface, indicating complete substrate coverage. The S 2p peaks broaden but stay intense with increasing Cr deposition. The presence of metallic Mo along with the persistence of S show that some interfacial chemistry has occurred. Annealing to moderate temperatures (750K) causes more extensive reaction than observed at room temperature, as a strong metallic Mo peak is detected along with several different S species. This reactivity is more extensive than observed for the Fe/MoS_2 interface at similar temperatures, but complete reaction to form chromium sulfide is not observed as with Mn/MoS_2. The most likely scenario for reaction is the presence of a reacted interface indicated by the presence of metallic Mo. The Cr overlayer is dominantly metallic, with some S intermixed, and a large amount of S having diffused through the Cr film to its surface.

The implications for the Cr/MoS_2 interfacial reaction on adhesion are more difficult to foresee. The presence of a fairly significant interfacial conversion of MoS_2 to metallic Mo and free S would seem unfavorable. However, the lack of extensive, bulk formation of a chromium sulfide and the predominance of strongly adsorbed sulfur on the surface of the Cr film might indicate possible strong adhesion. The intermediate chemistry is the most difficult to categorize, and further investigations of its affect on tribological properties would certainly be of interest.

The relatively inert MoS_2 (0001) surface has no unsatisfied bonds with which metals can strongly interact upon deposition onto MoS_2. The reaction mechanism for the decomposition of MoS_2 by a metal likely proceeds via electron donation from the deposited metal atoms into the unoccupied, antibonding molecular orbitals that are predominantly located on the Mo ion and are not easily accessible through the (0001) plane. These orbitals are also covalently mixed with the S 3p orbitals as discussed previously, but the spatial extent of the S portion of the $2e'$ and $2e''$ antibonding orbitals above the (0001) plane, where the greatest overlap with the deposited metal s and d-orbitals would occur, is unknown. The presence of a sulfur vacancy on the (0001) plane or an edge-plane site would permit the direct interaction of the deposited metal with the Mo 4d-based MOs. Once electrons have entered the antibonding levels, the Mo-S bonds would be weakened, allowing the reaction to proceed. The evaporation of relatively hot metal atoms onto MoS_2 could possibly induce defects to form and help initiate a reaction.

The likelihood that a deposited metal atom will donate electrons to MoS_2 probably depends on two factors: orbital overlap and the tendency of the metal to donate electrons. It is unlikely that

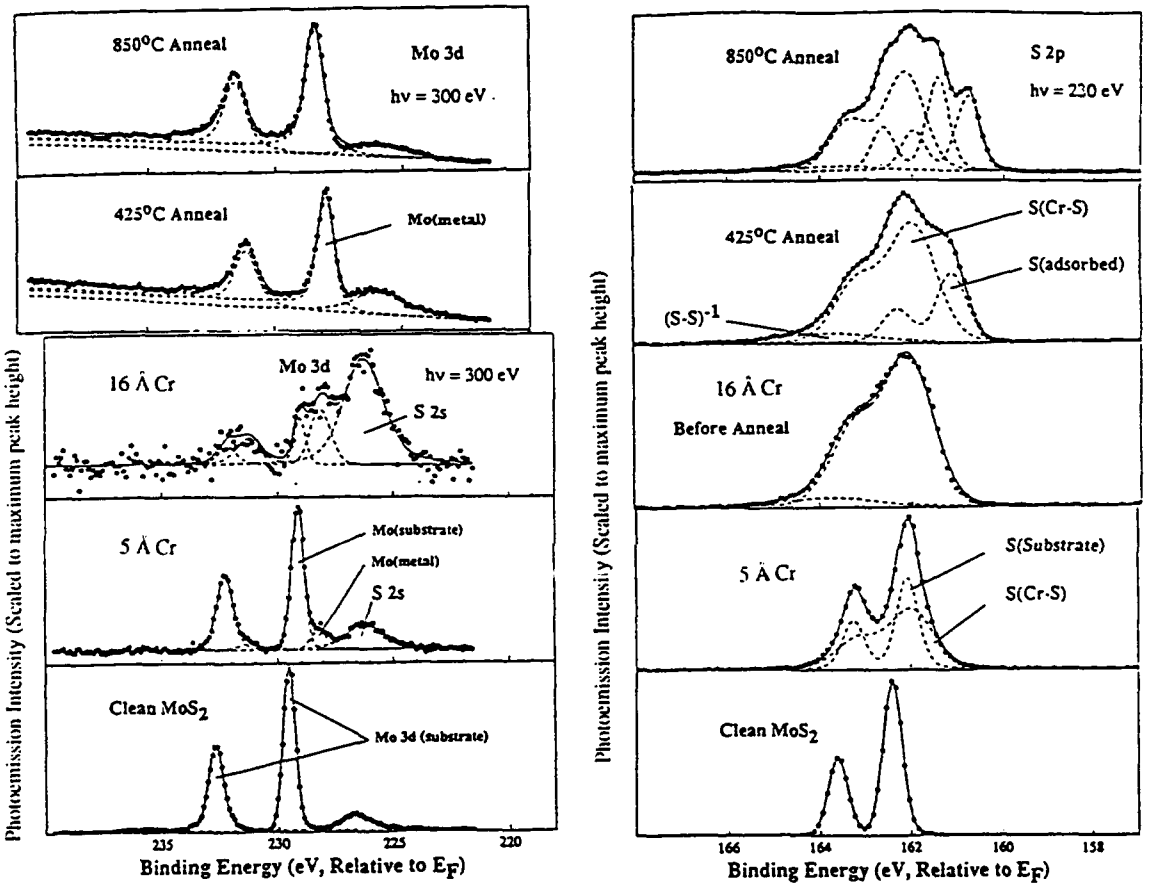

Figure 10. The Mo 3d (left) and S 2p core levels of MoS_2 obtained as a function of Cr-metal deposition and subsequent anneals. Even though significant metallic Mo is evident in the data, the Cr 3p peaks (not shown) did not indicate wholesale formation of CrS.

atoms of the various metals examined in the work described here have significantly different orbital overlap with MoS_2. In addition, the ionization potential of the transition metal atoms generally increases with increasing atomic number (Cr: 6.77 eV; Mn: 7.44 eV; Fe: 7.87 eV) [71], a trend which is not in agreement with the reactivity observed. The clustering of metal atoms to form a more metallic species than exists for the isolated atom may be required to permit the facile donation of electrons. Indeed, more extensive reactivity is detected by PES for all three metals with increasing surface coverage. The work function of a metal is always lower than the ionization potential of the metal atom, indicating that an electron is more easily removed from a cluster than an isolated atom. For the metals studied in this work, the work function trend does agree with the differences in reactivity (Mn: 4.1 eV; Cr: 4.5 eV; Fe: 4.5-4.8 eV) [71]. The relative ease of electron transfer must be directly related to the reaction activation energy, with the Mn reaction occurring most readily. Naturally, the thermodynamic stability of the reaction products also plays an important role in this chemistry, and the trend in reactivity for these three metals does mirror the trend in Δ .

From a technological point of view, several commercially available MoS_2 lubricant films use co-sputtered or sequentially sputtered metals to change film growth and morphology patterns. In particular, relatively unreactive metals such as Au, Ni, and Pb have been used in MoS_2 films, creating structural effects without decomposing the lubricant. These effects will be discussed in more detail in Section 4.

In the real world of thin-film application of MoS_2 lubricants, the steel or other substrate provides nucleation sites for film growth. In some cases (ultra-high vacuum deposition, substrate sputter cleaning), metallic species may indeed be present at the surface to initiate reactions or just provide sites for adhesion. The above studies should be very helpful in understanding the reactions taking place under such conditions. Most deposition processes, however, are not nearly as clean and well controlled as the detailed single-crystal data. In general, parts to be coated have been exposed to the environment and subjected to various levels of ex-situ and in-situ cleaning. Another major difference in film deposition chemistry is the reactive nature of the MoS_2 species in the plasma, where the MoS_2 fragments of unknown type are certainly more reactive than the (0001) basal plane. The next topics to be covered in this work are the nucleation, growth, and structure of sputter-deposited MoS_2 films and the relationship between substrate surface chemistry and film growth.

4. MoS_2 FILM GROWTH AND STRUCTURE

The original use of MoS_2 as a lubricant involved the burnishing of the powder material onto one or both of the contacting surfaces. Sometime later, bonded-solid-lubricant films became available in which MoS_2 and other "pigments" were suspended in a polymer or glass-forming matrix that acted to hold the lubricant in the desired location. (See the review article by Winer [72].) Such films were tens of micrometers thick, so their use in any precision application required considerable running in (or preburnishing) followed by cleaning and adjustment of dimensions to compensate for lost material due to wear. Furthermore, the binder material from bonded-solid-lubricant films often became loose debris that interfered with smooth operation of precision parts. Consequently, these materials were not highly regarded for high-reliability space applications, and solid lubrication was generally disdained by spacecraft designers, except for very-low duty cycle, generally sliding type devices such as release and deployment apparatus.

The formation of binderless, smooth, sub-micrometer-thick films of MoS_2 by means of sputter-deposition, first introduced by Spalvins [73], opened a variety of new possibilities for solid lubrication of high-tolerance parts and, at the same time, raised many questions regarding the physical and chemical mechanisms by which these films provide effective lubrication. Sputter deposition had been developed primarily for use in the semiconductor industry for providing controllable layers in integrated circuit chips but was a natural method of producing the binary compound material, MoS_2, in thin-film configurations. Under proper operating conditions, the sputtering process generally maintains the chemical composition of the target in the deposited film, and the decomposition of MoS_2 rather than its evaporation or sublimation precluded use of the more conventional physical vapor deposition techniques.

Initial investigations of sputtered MoS_2 films followed the classical pattern of putting coatings on parts or coupons and measuring friction, wear, and endurance [74-77]. Concurrently, surface analysis and microscopy of as-deposited [18,74,78-80] and worn films [8,81] revealed the defect-ridden, oxygen-contaminated character of the typical films. As techniques for surface science and analysis have improved our abilities to probe to much finer atomic-level sensitivity (i.e., the availability of high spatial and energy resolution XPS, high-energy TEM, STM and AFM, and EXAFS), a greater understanding of the electronic and crystal structure(s) of MoS_2 films has been forthcoming. But, how can an improved understanding of the electronic structure of a material lead to a better knowledge of, and control of, its growth and use as a lubricant film? In the case of MoS_2, its anisotropic crystal structure is the direct result of the coordination adopted by the Mo in the surrounding cluster of S atoms, and this trigonal prismatic symmetry derives from the arrangement of electrons within the constituent molecular orbitals as described above. The important questions of how this crystalline structure and MO arrangement in MoS_2 determine the growth patterns and substrate-surface adhesion characteristics of its films will be discussed in this section.

4.1 MoS_2 FILM NUCLEATION

The hexagonal, platelet grouping of atoms in MoS_2 appears to be common to all sputtered films of this material, regardless of whether their macroscopic structures are ordered or not [82]. Even

"amorphous" films, by X-ray and TEM standards, have the basic hexagonal unit with 6 S nearest neighbors to Mo, as demonstrated by EXAFS (Extended X-ray Absorption Fine Structure) studies. One difference between the films and the more crystalline material is the absence of long-range order in the films. The radial distribution functions obtained using EXAFS on several different MoS_2 films are shown in Figure 11. It is evident by comparison to results from a crystalline MoS_2 powder that the peaks for the next nearest neighbors (second and higher shells) are not distinct in the films, demonstrating the absence of long-range order. A second feature observed in the EXAFS results of the films is that their "nano-crystals" contain varying amounts of oxygen substituted into the MoS_{2-x} phase in proportion to the amount of oxygen or water present during deposition [82-84]. While these variations in film composition and structure affect their lubricating abilities, as will be discussed in the next section, the important thing to notice here is that rather widely varying deposition conditions generally produce the same material, albeit with significant differences in S to Mo stoichiometry and in grain size and morphology. Such differences originate with the surface conditions of the substrate, specifically with the nucleation sites on its surface, and are further affected by the atmosphere during deposition. (Although not all films have been investigated with EXAFS, it is speculated here that essentially

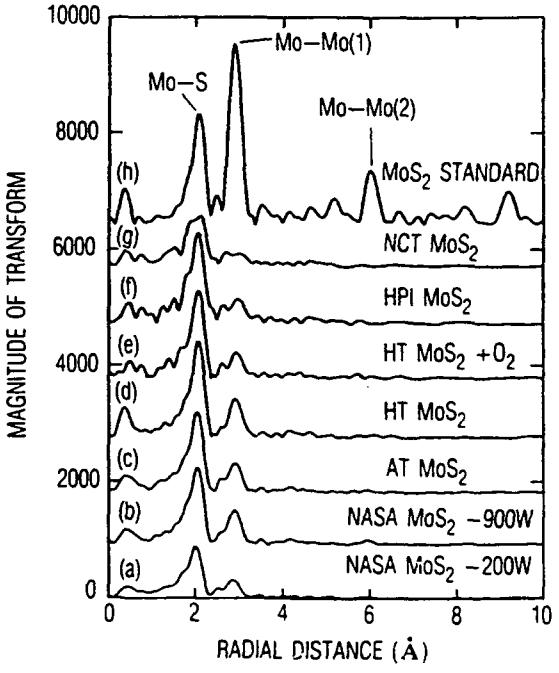

Figure 11. EXAFS radial distribution functions (RDF) for several different sputter-deposited MoS_2 films. A pure crystalline MoS_2 powder is provided for comparison. All films have a peak near 2 Å where the first Mo-S shell is expected. However, the RDF for each film also shows decreased intensity for peaks at larger distances representing atoms in the higher shells of coordination. The film data also reveal features associated with a new phase containing oxygen substituted for sulfur in a portion of the lattice. Reference 82 should be consulted for details regarding film preparation and chemical composition. (Reprinted with permission from authors of reference 82.)

all variations in S:Mo ratio in films, with the probable exception of those produced by ion-assisted deposition, are accompanied by compensating substitution of oxygen in the MoS_{2-x} lattice.)

Films of anisotropic materials, such as MoS_2, can grow with different orientations of the developing crystallites (in this case platelets). Initial islands of MoS_2 can be oriented with their (0001) basal planes parallel (basal islands) or perpendicular (edge islands) to the substrate [21]. It is clear from the increasing amount of data concerning growth on different substrates and at different stages of film development [19,21,85,86] that the thermodynamically preferred orientation is in the form of basal islands, but that the edge-island growth prevails, due to kinetic factors, if a nucleation site is provided. Such nucleation sites have been associated with hydroxyl groups [81], carbon-oxygen groups [82], defects in the MoS_2 itself [21], and with defects (steps or kinks) in the substrate that persist into the evolving film.[4] Basal islands are favored by removal of these active sites and growth under conditions of elevated temperature (≥ 200 °C), low system base pressure (i.e., low contamination), and relatively low sputtering gas pressure that is enriched with S-containing species (H_2S) to prevent S depletion [87]. These conditions provide for slow growth rates and the opportunity for diffusion on the surface during growth to allow development of the energetically favored configuration (orientation).

4.2 STEEL SURFACE CHEMISTRY

The final surface processing step prior to cleaning and lubrication for virtually any mechanical component made of steel is the honing or polishing to the desired surface finish. The chemical composition of the steel surface following this final polish plays a significant role in the adhesion of sputter-deposited MoS_2 films. To better understand the surface chemical bonding and reactivities of steels, we have used XPS to study two different steels after polishing in air. In addition, the effects on the surface chemistry of Ar^+ ion sputter cleaning as well as ex-situ cleaning of these materials have been addressed. Finally, the adhesion of sputter-deposited MoS_2 films on steel surfaces following the different cleaning processes will be presented.

The two steels examined in this work were 440C stainless (containing approximately 16 atomic % Cr) and 52100 bearing steel (1 to 2 atomic % Cr). The chemical composition of the surfaces of these materials was studied with XPS following polishing with diamond paste and alumina powder. The substrates were then subjected to one of three different cleaning processes: solvent cleaning with ethanol and acetone, very brief (< 1 min) etching with a 20% HCl/ethanol solution followed by an ethanol rinse, or 1-hr washes in a commercial alkaline cleaning solution (Alum etch 34, 15% in deionized H_2O; pH = 12.8) followed by water and ethanol rinses. The X-ray photoelectron spectrometer was a Surface Science Instruments X301 using a monochromatized Al Kα source with a 300-μm spot size and 50-eV pass energy. The energy resolution under these conditions produce a gold $4f_{7/2}$ peak width of 0.95 eV. The steel surface composition was studied in a variety of ways, including angle-resolved XPS and Ar^+ sputter profiling.

Steel surface chemistry has been studied by several groups [88], but the object of this work was to determine the composition and thickness of the oxide layer following the polishing and sample

[4] In Figure 4 of Ref. 19, a distinct step (possibly a dislocation) is evident in the substrate immediately below the point where the edge growth begins in the film.

cleaning. Figure 12 shows the Fe and Cr $2p_{3/2}$ XPS peaks from a 440C surface following solvent cleaning as a function of sample angle relative to the electron detector [11]. In each data set, the broad peak at higher binding energy is the result of photoemission from the metal oxide, while the sharper peak at lower binding energy shows the metallic species. By rotating the sample away from the analyzer, the technique becomes more surface sensitive as the effective escape depth of electrons through the solid is decreased. For both data sets (each has been normalized to the intensity of the oxide peak in the 0° data by multiplying by the factor listed near each spectrum), the metal peak decreases in intensity as the surface sensitivity is increased. Not surprisingly, this means that the oxide layers exist on top of the metallic species. The normalization factors for the Cr data at a given angle (other than 0°) are consistently and systematically larger than those for the Fe data. The larger factors required for the Cr data indicate that the chromium oxide photoelectrons are experiencing a greater attenuation by the surface layers and, hence, lay below the iron oxide species. This result is also consistent with an Ar^+ sputter profile of the 440C surface, which proved that iron oxide species are sputtered away first, followed by chromium oxide species [11,89]. The resulting picture of the 440C surface is shown in Figure 13, where the corrosion-resisting chromium oxide layer is below a surface iron oxide overlayer. Both layers are covered with an inhomogeneous, carbonaceous layer of contaminants remaining following the solvent cleaning. These contaminants were removed by a very brief sputter (< 1 min) but certainly can play a role in the steel surface chemistry if left intact.

The chemical composition of the solvent-cleaned 52100 steel surface is significantly different than that for 440C, consistent with the fact that 52100 is not a stainless steel and contains only 1 to 2% Cr. This material had an iron oxide overlayer that had approximately the total thickness of both oxide layers observed on 440C. A small amount of chromium oxide was dispersed in the iron oxide overlayer, but no corrosion-resistant layer was formed. However, the surface compo-

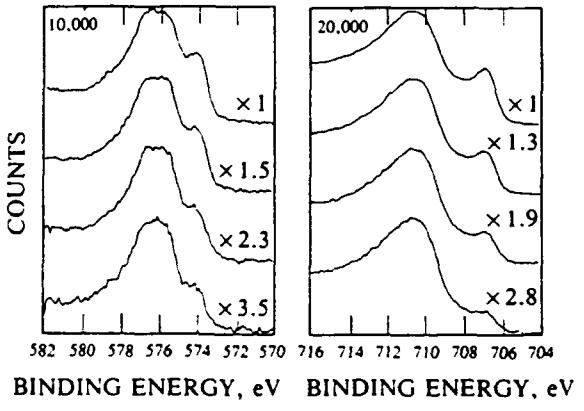

Figure 12. The Cr (left) and Fe $2p_{3/2}$ peak obtained with XPS as a function of sample angle relative to the analyzer central axis. From the top, the angles between the surface normal and analyzer entrance cone were 0°, 20°, 40°, and 60°. All data were normalized to the intensity of the higher binding energy, more intense oxide feature, and the normalization factors are listed on the figure. (Reprinted with permission from authors of reference 11. Copyright 1992, American Chemical Society.)

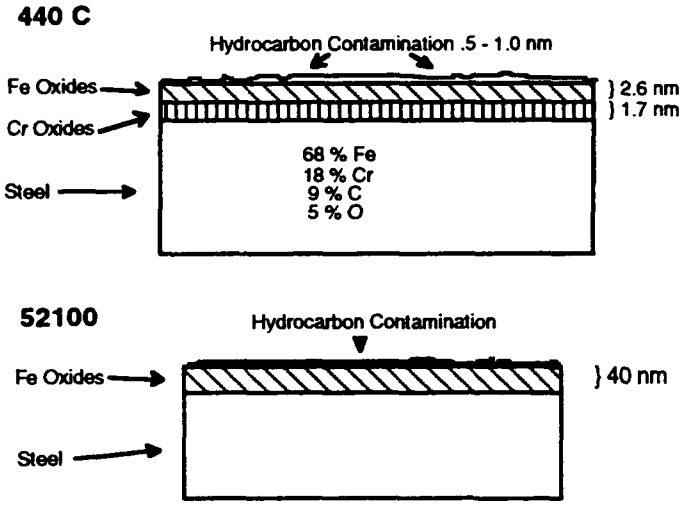

Figure 13. Schematic diagrams of the chemical compositions of 440C and 52100 steel surfaces. The oxide layer thicknesses are related to the specific sample handling procedures used in this work.

sition of 52100 steel is highly sensitive to sample handling, and the oxide layer can be much thicker if the material is allowed to corrode.

The effects of various surface treatments have also been studied with XPS [11,89]. It should be obvious that ion sputtering of the steels for sufficient periods of time will remove the surface oxide layers and allow solid lubricant films subsequently deposited to interact with metallic species. The background pressure of a deposition system, however, will control the actual surface composition of the steel, and if the material is allowed to stand in a relatively poor vacuum for an extended period following cleaning, then reacted surface layers will re-form. The effects of ex-situ sample cleaning varied with cleaning solutions and type of steel surface. Etches with the HCl/ethanol solution proved difficult to control for each steel. The results on the 440C surface following a 30-s acid etch are shown in Figure 14. Brief etches appeared to fairly selectively remove the iron oxide overlayer, leaving behind a dominantly chromium oxide surface. Etches for longer periods actually resulted in an increase in the iron oxide present when compared to the shorter etches. The surfaces also became pitted after the longer etches, indicating that both oxide layers had been penetrated and corrosion was occurring. This effect was confirmed on the 52100 surface where HCl/ethanol etches of any duration increased the oxide layer thickness. The 440C chromium oxide underlayer, therefore, does provide some protection from acidic treatments, but care must be taken. The alkaline treatments proved much more gentle to both steels. For both the 440C and 52100, most of the iron oxide overlayer was removed by the 1-hr wash (Figure 14). No evidence of sample pitting was observed on any steel substrate following the alkaline cleaning.

The steel surface compositions determined by XPS have interesting implications for the nucleation, growth, and adhesion of MoS_2 films. The iron-oxide overlayer on 440C is not strongly

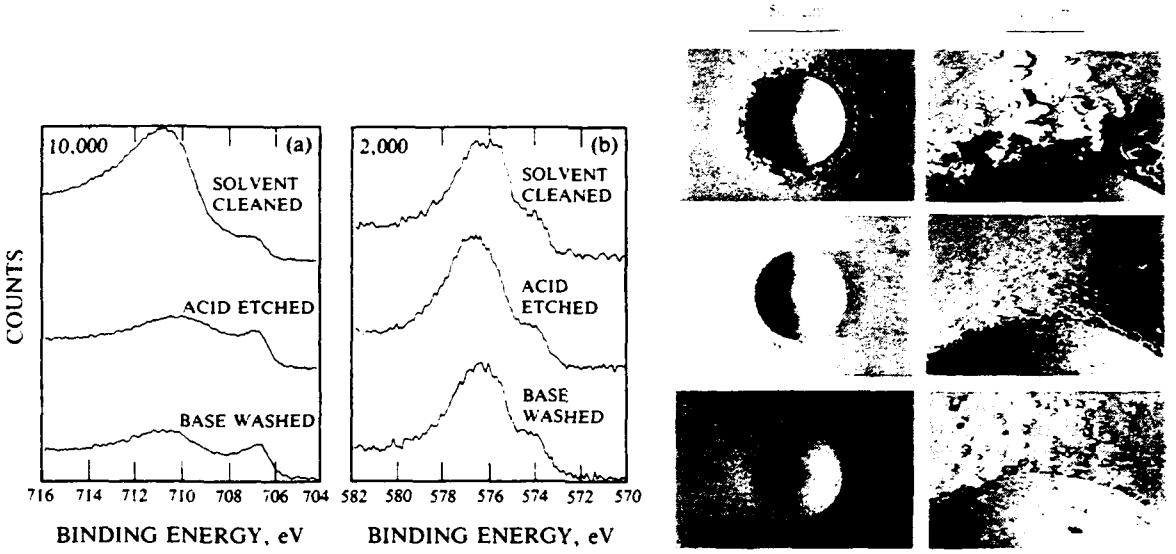

Figure 14. The Fe (left) and Cr $2p_{3/2}$ XPS peaks of 440C stainless as a function of ex-situ sample cleaning treatments along with SEM micrographs of MoS_2 film delamination experiments on similarly treated surfaces. The chemical treatments remove most of the iron-oxide overlayer and enhance adhesion and/or fracture toughness of the MoS_2 on the steel surfaces. (Reprinted with permission from reference 11. Copyright 1992, American Chemical Society.)

bonded to the bulk steel, but rather exists on top of the chromium oxide layer. The relative ease with which this layer is removed by chemical treatments indicate that it may not provide for strong adhesion of a solid lubricant film. Alternatively, the iron oxide of the 52100 steel is directly bonded to the bulk steel, but its potentially varying thickness depending on sample treatment make its mechanical reliability as a substrate questionable. The oxide layer on 52100 can be quite thick and loosely held by the substrate if large-scale corrosion is allowed to occur. In general, MoS_2 bonding to oxide surfaces should differ significantly from that on metallic surfaces because there are fewer free electrons available to react with the film. The nature of the surface bonding and reactivity of MoS_2 with oxides has not been explored in detail, but oxide ions are known to substitute for sulfide ions in the crystal structure of sputter deposited films [90] and, thus, could act as nucleation sites for edge-island growth.

The effects of the ex-situ removal of the iron-oxide overlayers on the bonding of MoS_2 lubricant films would seem problematic because the samples were exposed to air during introduction into the deposition chamber and were pumped down overnight to the 1×10^{-6} Torr base pressure. To determine if the ex-situ cleaning had an effect on lubricant adhesion, films deposited at ambient temperature on the differently pretreated surfaces of 440C were studied with an indentation test. The results of these tests are also shown in Figure 14, where SEM micrographs of 1-μm-thick films are shown on differently treated 440C following indentation with a Rockwell hardness tester. The films deposited on the acid- and base-treated surfaces adhere more strongly than on the solvent-cleaned 440C surface, which shows extensive film delamination around the indentation. Although the actual details of the interfacial chemistry have yet to be uncovered, we believe that the effects

are predominantly chemical in nature. Possibilities for the enhanced adhesion to the treated surfaces are that the MoS_2 films adhere strongly to the chromium oxide layer, the removal of the iron oxide overlayer may provide a more robust steel surface, the chemical treatments may have provided active sites for strong adhesion, or the thinner oxide layer might actually be removed or chemically reduced during the deposition process, allowing interaction with metallic species. In-situ ion etching of a steel substrate to remove the oxide layer results in a similar enhancement of MoS_2 film [91]. To further study substrate adhesion, the interaction of MoS_2 films on Si ceramic surfaces have been studied since these materials provide more well-defined and controllable surface chemical environments for handling than do the more reactive metals.

4.3 MoS_2/SILICON CERAMIC INTERACTIONS

Detailed studies concerning the nucleation and growth of sputter-deposited MoS_2 have been conducted on Si and SiC surfaces. For each material, the surface chemical composition was considered as a function of sample treatment and film deposition conditions. The crystallographic orientation of the growing MoS_2 films was followed by X-ray diffraction, which was used to determine which crystallographic planes were growing parallel to the substrate surface. The films to be discussed were grown at both ambient temperature (AT; 70°C) and high temperatures (HT; 220°C), with the HT films generally being more crystalline.

Single-crystal Si samples with oxide layers of varying thickness were initially studied [85]. Thin (2000 Å) MoS_2 films deposited at high temperature or at ambient temperature following a high-temperature surface anneal were found to grow with MoS_2 crystallites oriented with their basal planes parallel to the substrate. Alternatively, 2000 Å AT films grown without a surface thermal treatment grew with basal planes oriented perpendicular to the substrate surface. The principal effect of the high sample temperature is the removal of surface adsorbates, primarily hydrocarbons and water. This work led to an active site model for MoS_2 film nucleation and growth, where reactive surface species (believed to be H_2O or -OH on the SiO_2 surfaces) caused the MoS_2 crystallites to nucleate via an edge-plane site and grow with basal planes perpendicular to the surface. Removal of the active sites causes the MoS_2 to adopt a lower free energy orientation with the basal planes oriented parallel to the substrate surface. These effects have been beautifully documented by Moser and Lévy in TEM studies [19].

Similar studies were conducted on polycrystalline, hot-pressed SiC surfaces that were subjected to various ex-situ cleaning processes [86]. The chemical treatments were conducted in a nitrogen-purged glove bag and included methanol rinses, buffered HF etches, buffered HF followed by concentrated HNO_3 etches, and an ultrahigh vacuum anneal. XPS studies of the different samples showed that the HF etch removed the surface oxide along with surface contaminants, the HNO_3 etch removed more of the surface contaminants, and the UHV heating further desorbed carbon-containing contaminants (particularly C-O species). The orientation of HT MoS_2 films grown on these surfaces was highly dependent on surface treatment. In general, the cleaner the sample prior to introduction into the deposition system, the more MoS_2 was observed with basal planes oriented parallel to the substrate. These results are entirely consistent with the active site model proposed for the oxidized silicon surface, but the active sites appear to be C-O surface species on SiC. The effects of the various surface treatments on the tribological properties of the MoS_2 films will be discussed below.

One interesting implication of this work is that adhesion of MoS_2 to the silicon ceramics appears to be decreased by sample cleaning (implied by the basal orientation of the film near the interface), while adhesion to steels is enhanced by surface cleaning. This result may be controlled by the relative surface reactivities of the two materials since the silicon ceramics are thought to be relatively inert, particularly if a silicon oxide layer exists to passivate the surface. In addition, the orientation of the MoS_2 basal planes parallel to the substrate surface should result in a lower friction surface, a desirable result if sufficient surface adhesion exists for these films.

All of the controlled crystallite orientation studies have been conducted with nonmetallic or unreactive (gold) substrates, most of which have not been widely useful tribologically. (The silicon dioxide surfaces are typical of the type of atmospherically equilibrated surface one obtains with Si_3N_4, a promising bearing material with as yet very little practical application.) However, occasionally there have been instances of basal island growth on steel surfaces, which might signify operational possibilities if the proper surface preparation conditions can be devised [92-94]. The previous discussion of the reactivities of the metals iron, manganese, and chromium with the basal surface of MoS_2 is pertinent to our understanding of the proper conditions for such ordered growth. Recall that it is necessary to achieve basal orientation, but it is not sufficient; there must also be strong adhesion of the initial monolayers to the load-bearing substrate for a high probability of long endurance.

In an earlier article [6], we speculated that one way to obtain adhesion of basal planes to substrates would be to provide atoms on the substrate that could substitute for S in the MoS_2 basal plane and provide a "linkage" effect between metals. It was further speculated that such a linking atom would have to be one that could be multiply coordinated, as in an octahedral configuration, so that it could bond to three Mo atoms and a like number of substrate atoms. Some nonmetallic candidates were suggested as possibilities. In view of the surface reactivity studies involving Fe, Cr, and Mn, it now seems likely that for bare stainless steels Cr can provide the appropriate chemical interaction. A successful bonding agent would need to be able to substitute into the MoS_2 basal plane but not decompose the bulk material. Fe is unreactive; Mn is too reactive. Cr may have the proper balance of the ability to alloy with Mo but not drive the system to form bulk chromium sulfides [13,70].

In order to achieve such chemical bonding, the surface must be scrupulously clean, and metallic atoms must be available for "reaction." Controlled etching in inert environments is a practical and expedient pathway to obtain the proper substrate preparation [21,82]. In the case of ion etching, a common procedure prior to deposition, it is not sufficient to bombard in a contaminated (O_2, H_2O) environment because the contaminants will react with the substrate before the MoS_2 is deposited. The system base pressure must be low enough to maintain the reactivity of the prepared surface. Ion etching in contaminated environments will also improve adhesion by creating reactive bonding sites on oxide layers, but the orientation of the resultant film will be characteristic of edge-island growth.

4.4 FILM GROWTH MORPHOLOGY

The same system variables that influence the degree of edge-island versus basal-island nucleation, discussed in the preceding section, also control the morphologies of bulk film growth. Specifically, contaminants in the background gas, such as water vapor and carbon-oxygen com-

pounds, can provide nucleation sites for continued edge-island growth, but properly selected dopants that adsorb to the edge faces of evolving platelets and poison growth, such as metals and graphitic carbon, can provide for controllable basal-island growth.

Film structures can be characterized according to the zone model for growth and morphology [21]. Early films, and those produced in relatively uncontrolled vacuum environments with unconditioned targets, consisted of a thin compact region close to the substrate (~200 nm thick) covered by a very porous columnar region that was alleged to be essentially useless for lubrication [95]. Proper target conditioning, which involves multiple, sequential sputter runs, with rigorous control of the environment, followed by insertion of the substrates to be coated, is required to obtain basal orientation from a conventional compound MoS_2 target [8]. In contrast, such ordered films can be produced readily with reactive sputtering (H_2S) and an Mo metal target [87,96]. Buck [18] has explained these phenomena in terms of the competition of water vapor with the arriving MoS_2 during the deposition step. H_2O adsorbs onto edge planes of MoS_2, but rather than poison the surface for grain growth, it provides increased reactivity for continued nucleation. In a manner similar to the mechanism proposed by Gardos [97] for the effect of water on friction, namely the bonding of adjacent edge planes to form large platelets, adsorbed water enhances the growth of columnar structures. Excess water provides so many nucleation sites that the films do not have time to develop long-range order, and "amorphous" structures result.

To digress briefly, all of these growth patterns are determined by surface processes during film deposition. Although direct experimental proof of many of the following points is not available, there are observations and data for which this line of reasoning seems to be the only acceptable one. Furthermore, this discussion is based on sound fundamental surface-chemical principles. Adsorption of growth nuclei or poisons on edge surfaces, the most surface active or energetic ones, controls the ultimate morphologies of the films. In the above-mentioned case of reactive sputtering or for high-rate deposition, the S-containing species are in abundant excess over the moisture so that they arrive on the growth plane before collisions of H_2O occur. H_2O is effectively displaced from the growing film surfaces, and edge-island nucleation is suppressed. If a compound MoS_2 target is used, and it is not sufficiently conditioned to remove H_2O adsorbed on all of the surfaces within the compacted powder (grain boundaries), then this moisture is sputtered along with the MoS_2, and oxygen is incorporated into the film. The level of preconditioning (outgassing) will determine the concentration of oxygen contamination in the film. Some oxygen substitution in the MoS_{2-x} lattice may be advantageous as discussed below, but too much produces poorly ordered films that exhibit inferior wear properties. The adsorption of certain metals, such as Ni or Au, onto edge planes of platelets presents a relatively inert surface that appears to favor basal island growth [85,93]. By alternating thin ($\leq$ 10 nm) MoS_2 layers with very thin (< 1 nm) layers of relatively unreactive metals, a continuously renewed, clean surface for basal island growth is generated. In addition, the layering technique limits the size of lubricating crystallites/particles in the film, resulting in a dense, predominantly basal-oriented structure. To ensure these film properties, this technique requires a clean system (low background pressure) to prevent oxygen contamination.

It has been demonstrated that, upon use, MoS_2 films are deformed to create basal orientation and shear normal to the (001) crystallographic direction, regardless of the original growth orientation [91]. Why, then, is it important to have films with basal orientation during growth? The answer probably is that for long sliding or rolling life, the important issue is to have a very dense film

structure with as little porosity as possible. Such a film could have edge-island orientation, initially, providing that the crystallites were as small as possible (in the range of 5 to 10 nm on a side) so that very dense packing could occur. In practice, once edge growth begins from nuclei on the substrate or defects in the growing film, these platelets grow into columns that become wider as they develop outward from the substrate surface. Any basal platelets are shadowed from the incoming flux of material by the columns and gaps or pores form near the bases of the columns. (The pores are typically ≤ 50 nm in diameter, while the columns can be > 100 nm tall and 30 to 50 nm in diameter.) During use, such columns are typically sheared off at their bases forming debris that is only beneficial (as a lubricant) if it is trapped between the contacting surfaces. The lubrication regime for such entrapment is much like that for a burnished film, only with very small lubricant particles. Conversely, for very dense films with very small platelets, extremely thin layers of material are deformed during wear, and the material is lost gradually instead of in large columns. Films with basal orientation have near-theoretical densities and provide the optimum situation for wear as long as the adhesion is good, as described in the previous section. An added advantage of basal orientation is that there is a very small percentage of edge-plane facets, so the films are relatively unreactive and unaffected by contaminants (primarily moisture) during storage prior to use. Dry or vacuum environments are still required during operation with these films because the shearing action of the wear process exposes reactive edge facets that are easily oxidized, resulting in higher friction and severe wear.

5. TRIBOLOGICAL STUDIES

5.1 FRICTION AND WEAR TESTING

Two questions have been debated with respect to tribological (friction and wear) studies of lubricants for as long as such studies have been conducted. The first is whether friction and wear tests really provide any useful information for most applications of lubricants, namely in rolling-element bearings. The second is whether the "pin-on-disk" test has any validity for these same applications. Our experience is primarily with high-precision spacecraft mechanisms, but we suspect that similar circumstances pertain to other fields as well. An easy response to these questions is that there are numerous sliding applications in space mechanisms, such as many deployment devices, alignment mechanisms, and sliding sleeves (bushings) like telescoping booms for antennas or remote sensing instruments (e.g., the remote manipulating arm of the space shuttle). However, a more useful response is that the validity of a test is usually related to the type of motion in the application to which the test is being compared. Our experience is that many tests, including pin-on-disk or such modifications as thrust bearing life tests, are very good for ranking different lubricants or lubricant preparations, as in the case of solid films. Figure 15 shows that a reasonably good correlation exists between sliding wear-test life and rolling life for a number of sputtered MoS_2 thin films [98]. While this correlation may not always pertain, one thing is sure: the test should be designed to simulate the type of contact and the potential transport phenomena for the lubricant as closely as possible.

Have we just contradicted ourselves? Not really. What we are saying is that for solid lubricant testing and evaluation, it is more important to simulate the contact geometry and the ejection or retention and reuse of lubricant debris than it is to ensure that the contact is rolling or sliding [91]. Typically, a precision ball bearing that requires very low torque noise cannot rely on the transfer of lubricant from one surface to another, but must be lubricated with thin films on all surfaces, and the films must be tenacious enough to provide low friction for the entire life of the device. Other applications for which torque noise is not a critical parameter can operate with thick films and continuous transfer from surface to surface or with, for example, replenishment from sacrificial retainers that produce uneven, patchy films on the contacting surfaces but that can produce very long operating lifetimes.

It may also be that tribologists have become confused about the objectives of various tests, especially when debates rage about the validity of pin-on-disk tests. Most mechanism designers and builders would like to know how long a lubricant will last in their part. Most tribologists determine whether lubricant A outlasts lubricant B; they do not gather data that provide mechanism lifetime predictions directly. Tribological data must first be interpreted with the aid of a friction and wear model for the mechanism (part) of interest. Pin-on-disk tests provide very useful information on the friction and wear behavior of lubricants prepared under different conditions. Based on such data one can usually decide which lubricant will give the longest life with the lowest average friction. But, one will not get much useful information concerning friction (torque) noise for a ball bearing application, nor will one be able to calculate an operational life for a

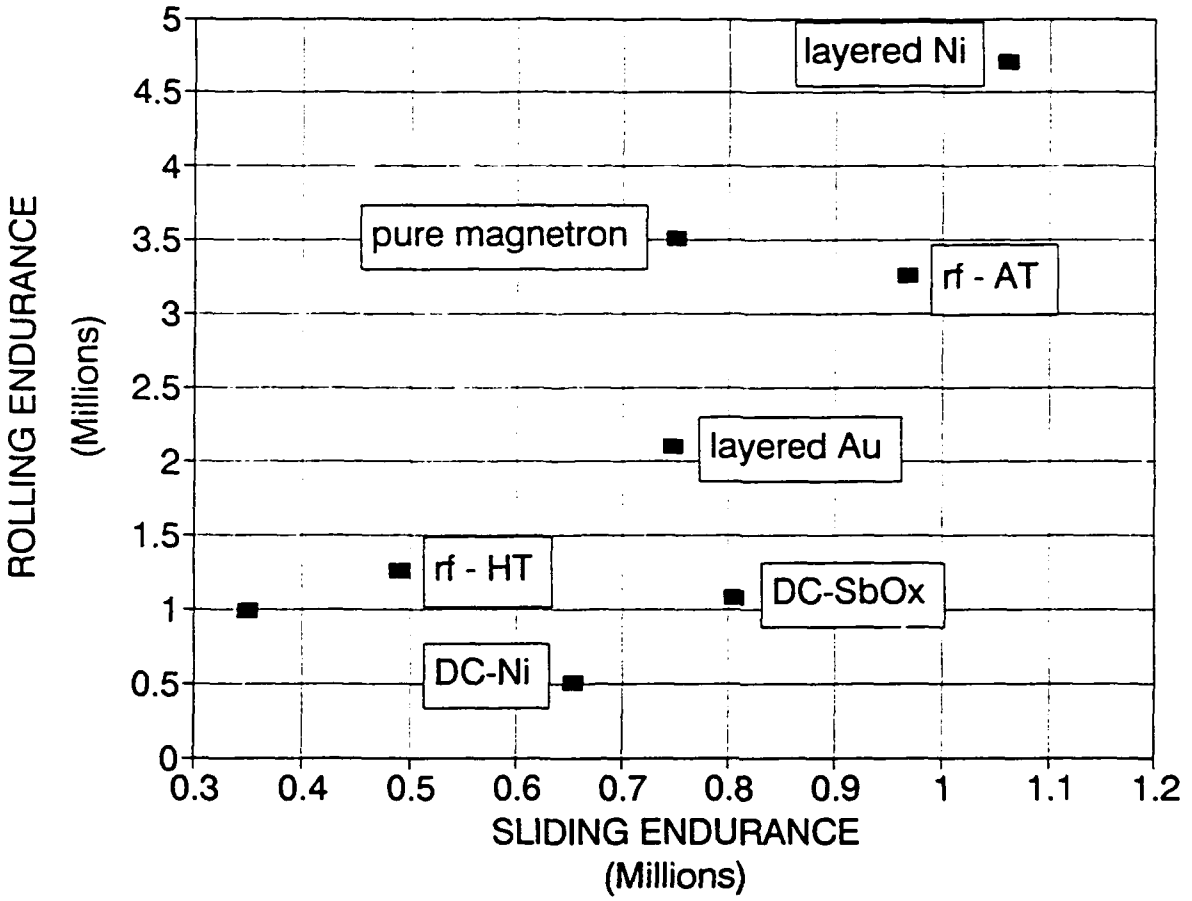

Figure 15. The correlation between sliding wear lives obtained from a thrust washer test to rolling wear lives from a thrust bearing test for various MoS_2 films. The films tested included the undoped AT and HT films discussed elsewhere in this report, along with various doped films prepared either by layering (layered Ni, layered Au) techniques or by co-sputtering (DC-Ni, DC SbO_x). Reference 98 should be consulted for more detail regarding this work.

specific mechanism without some benchmark for comparison or a model for predicting the dependence of life on film wear rate.

5.2 MoS_2 FILM PERFORMANCE

The friction and wear performance of different sputter-deposited MoS_2 films has been studied by several research groups on various substrates. As mentioned above, pin-on-disk tests have dominated this field, although a semi-quantitative relationship between sliding and thrust bearing tests has been demonstrated. Naturally, film producers tend to modify their films to maximize performance in whatever tribological test they use to determine performance. For that reason, we will focus on only a few studies that have taken films that were produced in various ways and

subjected to standard tests. In addition, the relationships between the surface science studies discussed in previous sections to the tribological performance of these films are best demonstrated through these few examples.

In both sliding and rolling tests, very dense films, produced by the well-controlled incorporation of dopants or other means to suppress rapid edge-plane growth, generally show the longest wear lives in most test procedures [93,98]. This doping has been best accomplished by layering films in very clean deposition systems, as discussed earlier. However, the addition of dopants can have an adverse effect on the measured film coefficient of friction. In particular, films incorporating metals to poison edge-plane growth often display higher friction than identical films without the dopant, and the friction appears to scale with the amount of incorporated metal. This effect has been observed in both sliding [93] and rolling tests [98]. An understanding of the chemical reactivity of MoS_2 with various metals should allow an intelligent selection of metal dopants, namely, an unreactive metal that also possesses some reasonable tribological behavior. Not surprisingly, gold and lead have become the two best candidates for metal dopants in MoS_2 films.

Earlier tribological work on MoS_2 revealed an interesting correlation between the stoichiometry of the film and low friction [79]. In this work, it was determined that films that were sulfur deficient (up to a limit) had lower friction than more stoichiometric films. At that time, the substitutional capabilities of oxygen into MoS_2 had not been realized, and we believe that the substoichiometric films actually contained a significant amount of substitutional oxygen. Obviously, if too much oxygen is incorporated, then the lubricant will begin to look more like an oxide and lose the ultra-low friction that MoS_2 provides. However, the incorporation of some oxide ions substituted for sulfide ions in the crystalline lattice does appear to be beneficial. The presence of oxide ions in the basal plane will obviously alter the interlayer and intercrystalline bonding forces. One could envision several results of this substitution, including greater local charge separation due to the more ionic Mo-O bond, a lessening of the surface polarizability, and changes in local bonding geometries. All of these effects would alter interlayer bonding forces. The greater charge separation would produce localized areas where greater Coulombic interactions would occur. The lowered surface polarizability would clearly reduce van der Waals interactions and decrease interlayer attractions. Changes in local geometry could alter electronic structure and bonding properties and disrupt the normal interlayer attraction. The net effect on the Madelung lattice energy of such a substitution would be an interesting problem, but the empirical observation of lower friction implies that interlayer repulsion is increased.

The MoS_2 films deposited on SiC surfaces discussed in Section 4 were also subjected to pin-on-flat testing [99]. The intent of these tests was to determine if the varying film orientation and adhesion resulting from the different surface pretreatments had an effect on friction and wear properties. Small but significant differences were indeed observed in these tests, with films deposited on acid-etched SiC displaying both lower initial friction and shorter lifetimes, consistent with the existence of more basal-oriented MoS_2 crystallites. This result emphasized the desire to produce basal-oriented films with enhanced surface adhesion properties. Alternatively, while the basal-oriented films had lower initial friction coefficients, the minimum friction coefficient during the tests showed no correlation to the amount of initial parallel basal-plane orientation.

5.3 LUBRICATION MECHANISM

Lubricant film structure and morphology will be the primary variables for the determination of wear life and also of noise during operation. MoS_2 films are deformed during use, and in many cases 80% to 90% of the film mass is worn away in the first 10% to 20% of life. However, some material selection is possible that results in longer service life, and this selection is accomplished through control of the surfaces of the lubricating particles. The actual type of surface control and the selection of film structure for a specific application depends, in part, on the nature of the basic physical mechanism by which the MoS_2 provides lubrication. In early literature, the issue was raised as to whether lubrication by MoS_2 consisted of intracrystalline cleavage along basal planes of individual particles (platelets) or intercrystalline sliding of particles over each other [72]. A seemingly ever-increasing data base indicates that the dense, low-porosity films give the best service life and suggests that the intercrystalline mechanism is the correct one for sputter-deposited films [10]. Furthermore, the smaller the particle size in a film, the better are the overall lubrication characteristics (stability of friction and length of operation).

Additional support of the intercrystalline slip mechanism is provided by the surface phonon dispersion for MoS_2 compared to that of the bulk material [16]. As discussed in Section 2, the external surface of MoS_2 has a structure slightly different from the "bulk" or internal surfaces of the basal planes and suggests that it should be easier to slide particles over each other than to cleave a single particle. If small particles (platelets) of MoS_2 slide over each other during rolling or sliding contact, then wear of the film would be associated with expulsion of these particles from the contact zone. It follows that for a given expulsion rate, the least wear would be obtained for expulsion of the smallest possible particles. Experimental determination of the optimum particle size has not been possible, but the results of two fundamental studies provide some insight into the small size limit for particles that still provide effective lubrication. The first study concerning EXAFS results for a number of sputter-deposited MoS_2 films has already been discussed, and the data of Figure 11 show that for most films there is little crystalline order beyond the first Mo-Mo bond distance [82]. One might ask if this nano-structure is large enough to provide all of the materials properties of MoS_2. While an answer cannot be given for all properties, the second study on *ab initio* theoretical calculations of the electronic structure of MoS_2 and comparison to photoelectron spectroscopic data indicates that the smallest "cluster" of the material that gives acceptable calculated energy levels is Mo_7S_{24} [46]. More realistically, in order to maintain stoichiometry and charge balance, the smallest crystalline structure would likely have the $Mo_{12}S_{24}$ cluster.

There is internal consistency among these results. This small cluster would allow a majority of the Mo atoms to have their complete set of nearest neighbor S atoms, while only a portion of the Mo-Mo first nearest neighbor and virtually none of the higher shell interaction would occur, which is exactly the situation observed in the EXAFS results of most sputter-deposited films. In addition, the agreement of calculated electronic energy level spacing for the Mo_7S_{24} with the valence level peaks in the photoelectron spectrum is quite good. An $Mo_{12}S_{24}$ cluster is depicted in Figure 16 along with the appropriate dimensions listed in the caption. Admittedly, there is no proof that such nano-platelets exist or that they are responsible for lubrication, but this cluster size probably represents the theoretical lower limit in actual crystalline size that might be expected to be effective.

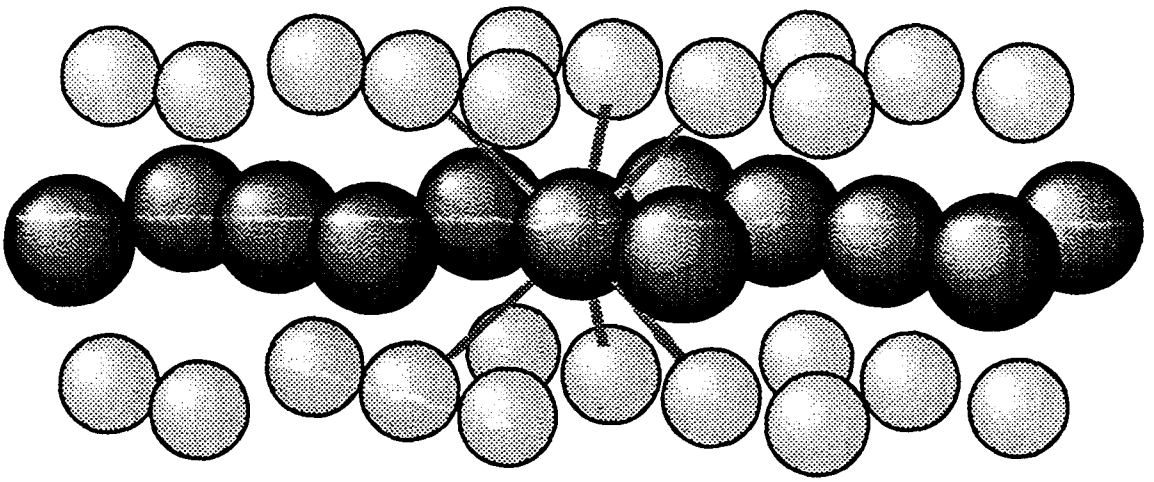

Figure 16. The $Mo_{12}S_{24}$ "nano-crystallite" that contains the smallest unit capable of reproducing the MoS_2 electronic structure in *ab initio* calculations (Mo_7S_{24}). The $Mo_{12}S_{24}$ cluster would be approximately 11 to 12 Å in diameter. In this figure, the Mo atoms are represented by the larger, darker-shaded spheres.

6. SUMMARY

In this report, we have explored several of the surface and interfacial interactions present in a solid lubricated tribological system. The various surface science techniques discussed have revealed the fundamental electronic structure and bonding properties within and between MoS_2 crystallites, the reactivity of MoS_2 with various metals that are important both for adhesion of a lubricating film to a substrate and in growing doped films, and the nucleation and growth of solid lubricating films resulting in various macroscopic film structures. In turn, many of these properties were shown to influence the friction and wear properties of MoS_2-based solid lubricants. Our intention has been to start with the most fundamental of chemical bonding interactions occurring in MoS_2 and build to an understanding of the practical use of this material as a solid lubricant needed for space-based applications. The use of surface science has played and continues to play a vital role in understanding solid lubrication and maximizing the lubricating potential of MoS_2.

REFERENCES

1. E. R. Braithwaite, *Solid Lubricants and Surfaces* (Pergamon Press, New York, 1964), p. 27.

2. M. N. Gardos, "Determination of the Tribological Fundamentals of Solid Lubricated Ceramics," Vol. 1: Summary, WRDC-TR-90-4096, November 1990, p. 5.

3. J. K. Lancaster, in *Handbook of Lubrication*, Vol. II, E. R. Booser, ed. (CRC Press, Boca Raton, FL., 1984), pp. 269-290.

4. F. P. Bowden and D. Tabor, *The Friction and Lubrication of Solids* (Oxford University Press, London, 1954), p. 1.

5. J. L. Lauer and B. G. Bunting, *Tribol. Trans.*, **31** (1988) 338.

6. P. D. Fleischauer, *Thin Solid Films*, **154** (1987) 309.

7. P. D. Fleischauer, J. R. Lince, P. A. Bertrand, and R. Bauer, *Langmuir*, **5** (1989) 1009.

8. P. D. Fleischauer and R. Bauer, *Tribol. Trans*, **31** (1988) 239.

9. M. R. Hilton and P. D. Fleischauer, *Mat. Res. Soc. Symp. Proc.*, **140** (1989) 227.

10. M. R. Hilton, R. Bauer, S. V. Didziulis, J. R. Lince, and P. D. Fleischauer, *Adv. Engin. Tribol.*, STLE Sp-31 (1990) 31.

11. S. V. Didziulis, M. R. Hilton, and P. D. Fleischauer, in *Surface Science Investigations in Tribology*, ACS Symp. Series No. 485, Y.-W. Chung, A. M. Homola and G. B. Street, eds. (American Chemical Society, Washington, D. C., 1992) pp. 44-57.

12. M. R. Hilton, R. Bauer, and P. D. Fleischauer, *Thin Solid Films*, **188** (1990) 219.

13. T. D. Durbin, J. R. Lince, and J. A. Yarmoff, *J. Vac. Sci Technol.*, **A 10** (1992) 2529, and references therein.

14. J. R. Lince, S. V. Didziulis, D. K. Shuh, T. D. Durbin, and J. A. Yarmoff, *Surface Sci.*, **277** (1992) 43.

15. S. V. Didziulis, J. R. Lince, P. D. Fleischauer, and J. A. Yarmoff, *Inorg. Chem.*, **30** (1991) 672.

16. P. A. Bertrand, *Phys. Rev.*, **B 44** (1991) 5745.

17. T. Spalvins, *Thin Solid Films*, **118** (1984) 375.

18. V. Buck, *Vacuum*, **36** (1986) 89.

19. J. Moser and F. Lévy, *J. Mater. Res.*, **7** (1992) 734.

20. J. Moser, H. Liao, and F. Lévy, *J. Phys. D: Appl. Phys.*, **23** (1990) 624.

21. M. R. Hilton and P. D. Fleischauer, *J. Mater. Res.*, **5** (1990) 406.

22. G. W. Stupian and M. S. Leung, *Appl. Phys. Lett.*, **51** (1987) 1560.

23. T. Ichinokawa, T. Ichinose, M. Tohayama, and H. Itoh, *J. Vac. Sci. Technol.*, **A 8** (1990) 500.

24. M. Weimer, J. Kramer, C. Bai, and J. D. Baldeschwieler, *Phys. Rev.*, **B 37** (1988) 4292.

25. C. M. Lieber and Y. Kim, *Thin Solid Films*, **206** (1991) 355.

26. Y. Kim, J.-L. Huang, and C. M. Lieber, *Appl. Phys. Lett.*, **59** (1991) 3404.

27. R. Coehoorn, C. Haas, J. Dijkstra, C. J. F. Flipse, R. A. deGroot, and A. Wold, *Phys. Rev.*, **B 35** (1987) 6195.

28. T. R. Coley, W. A. Goddard III, and J. D. Baldeswieler, *J. Vac. Sci.*, **B 9** (1991) 470.

29. C. Dellacorte and H. E. Sliney, *ASLE Trans.*, **30** (1987) 77.

30. J. C. McMenamin and W. E. Spicer, *Phys. Rev.*, **B 16**, (1977) 5474.

31. F. R. Shepard and P. M. Williams, *J. Phys. C: Solid State Phys.*, **7** (1974) 4427.

32. L. Ley, R. H. Williams, and P. C. Kemeny, *Il Nuovo Cimento*, **39** (1977) 715.

33. I. T. McGovern, R. H. Williams, and A. W. Parke, *J. Phys. C: Solid State Phys.*, **12** (1979) 2689.

34. I. Abbati, L. Braicovich, C. Carbone, J. Nogami, J. J. Yeh, I. Lindau, and U. del Pennino, *Phys Rev.*, **B 32** (1985) 5459.

35. I. Abbati, L. Braicovich, C. Carbone, J, Nogami, I. Lindau, and U. del Pennino, *J. Electron Spectrosc. Relat. Phenom.*, **40** (1986) 353.

36. J. R. Lince, S. V. Didziulis, and J. A. Yarmoff, *Phys. Rev.*, **B 43** (1991) 4641.

37. For example, see L. F. Mathiess, *Phys. Rev.*, **B 8** (1973) 3719.

38. U. Gelius and K. Seigbahn, *Far. Discuss. Chem. Soc.*, **54** (1972) 257.

39. S. Kono and T. Kobayashi, *Solid State Commun.*, **15**, 1421, (1974).

40. Adapted from J. J Yeh and I. Lindau, *At. Data Nucl. Data Tables*, **32** (1985) 1.

41. L. C. Davis, *J. Appl. Phys.*, **59** (1986) R25, and references therein.

42. C. M. Mate, G M. McClelland, R. Erlandsson, and S. Chiang, *Phys. Rev. Lett.*, **59** (1987) 1942.

43. N. Wakabayashi, H. G. Smith, and R. M. Nicklow, *Phys. Rev.*, **B 12**, 659 (1975).

44. B. J. Mrstik, R. Kaplan, T. L. Reinecke, M. van Hove, and S. Y. Tong, *Phys. Rev.*, **B 15**, 897 (1977).

45. S. V. Didziulis, S. L. Cohen, K. D. Butcher, and E. I. Solomon, *Inorg. Chem.*, **27** (1988) 2238.

46. T. B. Stewart, manuscript in preparation.

47. K. Chrissafis, M. Zamani, K. Kambas, J. Stoemenos, N. A. Economou, I Samaras, and C. Julen, *Mater. Sci. Eng.*, **B 3** (1989) 145.

48. M. Kertesz and R. Hoffmann, *J. Am. Chem. Soc.*, **106** (1984) 3453.

49. R. Hoffmann, J. M Howell, and A. R. Rossi, *J. Am. Chem. Soc.*, **98** (1976) 2484.

50. R. Huisman, R. De Jonge, C. Haas, and F. Jellinek, *J. Solid State Chem.*, **3** (1971) 56.

51. A. A. Golubnichnaya and V. L Kalikhman, *Proc. Acad. Sci. SSSR, Inorganic Materials*, **14** (1978) 228.

52. S. M. Davis and J. C. Carver, *Appl. Surf. Sci.*, **20** (1984) 193.

53. R. R. Chianelli, A. F. Ruppert, S. K. Behal, B. H. Kear, A. Wold, and R. Kershaw, *J. Catal*, **92** (1985) 56.

54. G. L. Montet, *Appl. Phys. Lett.*, **11** (1967) 223.

55. K. Siegbahn, et al., *Phys. Rev.*, **110** (1958) 776.

56. M. P. Seah and W. A. Dench, *Surf. Interf. Anal.*, **1** (1979), and references therein.

57. S. M. Davis and J. C. Carver, *Appl. Surf. Sci.*, **20** (1984) 193.

58. J. R. Lince, D. J. Carré, and P. D. Fleischauer, *Langmuir*, **2** (1986) 805.

59. H. C. Feng and J. M Chen, *J. Phys.*, **C 7** (1974) 175.

60. M. Matsunaga, T. Homma, and A. Tanaka, *ASLE Trans.*, **25** (1982) 323.

61. J. R. Lince, T. B. Stewart, M. M. Hills, P. D. Fleischauer, J. A. Yarmoff, and A. Taleb-Ibrahimi, *Surf. Sci.*, **210** (1989) 387.

62. D. A. Shirley, *Phys. Rev.*, **B 5** (1972) 4709.

63. G. K. Wertheim, S. B. DiCenzo, and S. E. Youngquist, *Phys. Rev. Lett.*, **51** (1983) 2310.

64. K. S. Liang, S. P. Cramer, D. C. Johnston, C. H. Chang, A. J. Jacobson, J. P. deNeufville, and R. R. Chianelli, *J. Non-Cryst. Solids*, **42** (1980) 345.

65. J. R. Lince, D. J. Carré, and P. D. Fleischauer, *Phys. Rev.*, **B 36** (1987) 1647.

66. J. R. Lince, T. B. Stewart, P. D. Fleischauer, J. A. Yarmoff, and A. Taleb-Ibrahimi, *J. Vac. Sci. Technol.*, **A 7** (1989) 2469.

67. T. Spalvins, NASA Technical Note, NASA TN D-7169, 1973.

68. J. R. Lince, T. B. Stewart, M. M. Hills, P. D. Fleischauer, J. A. Yarmoff, and A. Taleb-Ibrahimi, *Surf. Sci.*, **223** (1989) 65.

69. J. S. Zabinski and B. J. Tatarchuk, *Mater. Res. Soc. Symp. Proc.*, **140** (1989) 239.

70. T. D. Durbin, D. K. Shuh, J. A. Yarmoff, J. R. Lince, and S. V. Didziulis, manuscript in preparation.

71. R. C. Weast, ed., *CRC Handbook of Chemistry and Physics*, 64th Edition, (CRC Press, Boca Raton, FL., 1983).

72. W. O. Winer, *Wear*, **10** (1967) 422.

73. T. Spalvins, *ASLE Trans.*, **14** (1971) 267.

74. T. Spalvins, *Thin Solid Films*, **73** (1980) 291.

75. R. I. Christy and H. R. Ludwig, *Thin Solid Films*, **64** (1979) 223.

76. B. C. Stupp, *Thin Solid Films*, **84** (1981) 257.

77. E. Bergmann, G. Melet, C. Mueller, and A. Simon-Vermot, *Tribol. Int.*, (1981) 329.

78. R. Bichel and F. Levy, *Thin Solid Films*, **116** (1984) 367.

79. H. Dimigen, H. Hubsch, P. Willich, and K. Reichelt, *Thin Solid Films*, **129** (1985) 79.

80. P. D. Fleischauer, *ASLE Trans.*, **27** (1984) 82.

81. T. B. Stewart and P. D. Fleischauer, *Inorg. Chem.*, **21** (1982) 2426.

82. J. R. Lince, M. R. Hilton, and A. S. Bommannavar, *Surf and Coatings Technol.*, **18** (1990) 640.

83. V. Buck, *Wear*, **114** (1987) 263.

84. V. Buck, *Wear*, **91** (1983) 281.

85. P. A. Bertrand, *J. Mater. Res.*, **4** (1989) 180.

86. S. V. Didziulis and P. D. Fleischauer, *Langmuir* , **6** (1990) 621.

87. J.-Ph. Nabot, A. Aubert, R. Gillet, and Ph. Renaux, *Surf. Coat. Technol.*, **46** (1991) 629.

88. S. Jin and A. Arens, *Appl. Phys.*, **A 50** (1990) 287, and references therein.

89. M. R. Hilton, R. Bauer, S. V. Didziulis, and P. D. Fleischauer, *Thin Solid Films*, **201** (1991) 49.

90. J. R. Lince, *J. Mater. Res.*, **5** (1990) 218.

91. P. D. Fleischauer, M. R. Hilton, and R. Bauer in *Mechanics of Coatings*, Leeds-Lyon 16, Tribology Series 17, D. Dowson, C. M. Taylor, and M. Godet, eds., (Elsevier, Amsterdam, 1990), 121.

92. P. D. Fleischauer and L. U. Tolentino, *Proc. 3rd ASLE Int. Solid Lubr. Conf.*, ASLE SP-14,(1984) 223,

93. M. R. Hilton, R. Bauer, S. V. Didziulis, M. T. Dugger, J. M. Keem, and J. Scholhamer, *Surf. Coat. Technol.*, **53** (1992) 13.

94. R. Bauer, unpublished work.

95. T. Spalvins, *Thin Solid Films*, **96** (1982) 17.

96. A. Aubert, J.-Ch. Nabot, J. Ernoult, and Ph. Renaux, *Surf. Coat. Technol.*, **41** (1990) 127.

97. M. N. Gardos, *Tribol. Trans.*, **31** (1988) 214.

98. S. V. Didziulis, M. R. Hilton, R. Bauer, and P. D. Fleischauer, Aerospace Report No. TOR-92(2064)-1, The Aerospace Corporation, 15 October 1992.

99. S. V. Didziulis, P. D. Fleischauer, B. L. Soriano, and M. N. Gardos, *Surf. Coatings Technol.*, **43/44** (1990) 652.

TECHNOLOGY OPERATIONS

The Aerospace Corporation functions as an "architect-engineer" for national security programs, specializing in advanced military space systems. The Corporation's Technology Operations supports the effective and timely development and operation of national security systems through scientific research and the application of advanced technology. Vital to the success of the Corporation is the technical staff's wide-ranging expertise and its ability to stay abreast of new technological developments and program support issues associated with rapidly evolving space systems. Contributing capabilities are provided by these individual Technology Centers:

Electronics Technology Center: Microelectronics, solid-state device physics, VLSI reliability, compound semiconductors, radiation hardening, data storage technologies, infrared detector devices and testing; electro-optics, quantum electronics, solid-state lasers, optical propagation and communications; cw and pulsed chemical laser development, optical resonators, beam control, atmospheric propagation, and laser effects and countermeasures; atomic frequency standards, applied laser spectroscopy, laser chemistry, laser optoelectronics, phase conjugation and coherent imaging, solar cell physics, battery electrochemistry, battery testing and evaluation.

Mechanics and Materials Technology Center: Evaluation and characterization of new materials: metals, alloys, ceramics, polymers and their composites, and new forms of carbon; development and analysis of thin films and deposition techniques; nondestructive evaluation, component failure analysis and reliability; fracture mechanics and stress corrosion; development and evaluation of hardened components; analysis and evaluation of materials at cryogenic and elevated temperatures; launch vehicle and reentry fluid mechanics, heat transfer and flight dynamics; chemical and electric propulsion; spacecraft structural mechanics, spacecraft survivability and vulnerability assessment; contamination, thermal and structural control; high temperature thermomechanics, gas kinetics and radiation; lubrication and surface phenomena.

Space and Environment Technology Center: Magnetospheric, auroral and cosmic ray physics, wave-particle interactions, magnetospheric plasma waves; atmospheric and ionospheric physics, density and composition of the upper atmosphere, remote sensing using atmospheric radiation; solar physics, infrared astronomy, infrared signature analysis; effects of solar activity, magnetic storms and nuclear explosions on the earth's atmosphere, ionosphere and magnetosphere; effects of electromagnetic and particulate radiations on space systems; space instrumentation; propellant chemistry, chemical dynamics, environmental chemistry, trace detection; atmospheric chemical reactions, atmospheric optics, light scattering, state-specific chemical reactions and radiative signatures of missile plumes, and sensor out-of-field-of-view rejection.